

Explainable Artificial Intelligence: How Subsets of the Training Data Affect a Prediction

Andreas Brandsæter^{a,b,*}, Ingrid K. Glad^b

^a*Group Technology and Research, DNV GL, P.O Box 300, HØVIK, 1322, Norway.*

^b*Department of Mathematics, University of Oslo, Oslo*

Abstract

There is an increasing interest in and demand for interpretations and explanations of machine learning models and predictions in various application areas. In this paper, we consider data-driven models which are already developed, implemented and trained. Our goal is to interpret the models and explain and understand their predictions.

Since the predictions made by data-driven models rely heavily on the data used for training, we believe explanations should convey information about how the training data affects the predictions. To do this, we propose a novel methodology which we call Shapley values for training data subset importance. The Shapley value concept originates from coalitional game theory, developed to fairly distribute the payout among a set of cooperating players. We extend this to subset importance, where a prediction is explained by treating the subsets of the training data as players in a game where the predictions are the payouts.

We describe and illustrate how the proposed method can be useful and demonstrate its capabilities on several examples. We show how the proposed explanations can be used to reveal biasedness in models and erroneous training data. Furthermore, we demonstrate that when predictions are accurately explained in a known situation, then explanations of predictions by simple models correspond to the intuitive explanations. We argue that the explanations enable us to perceive more of the inner workings of the algorithms, and illustrate how models producing similar predictions can be based on very different parts of the training data. Finally, we show how we can use Shapley values for subset importance to enhance our training data acquisition, and by this reducing prediction error.

Keywords:

Shapley Values, Machine Learning Interpretation, Explainable AI, Data-Centric Explanations, Opening the Black-box

1. Introduction

We are surrounded by predictions, classifications and decisions made by algorithms and computer programs whose reasoning and logic are unavailable to us. Although the reasoning can sometimes be intentionally hidden from us, most of the time, it is unavailable due to the complexity of the systems and the models used. The algorithms can sometimes be simple enough, but after training on massive and complex datasets, the final models are often difficult to decipher and challenging to explain and interpret. Due to the models' inscrutable inner workings, such models are often labelled black-boxes (Hall and Gill, 2018). The behaviour of such models on an unseen dataset cannot be predicted, even by the people who develop and implement the algorithms and design the models.

The importance of transparency, explanations and interpretations of machine learning models is growing, particularly for decision making in safety critical systems (Kim

et al., 2016). Doshi-Velez and Kim (2017) argue that interpretations and explanations can be important to ensure safety since we often cannot create a complete list of training scenarios in which a system can fail. Ribeiro et al. (2016) claim that "if the users do not trust a model or a prediction, they will not use it". If we understand the model's reasoning, it is easier to verify the model and determine when the model's reasoning is in error, and to improve the model (Caruana et al., 1999; Doshi-Velez and Kim, 2017; Lundberg and Lee, 2017). Furthermore, transparency, interpretations and explanations can guard against unethical or biased predictions, such as discriminations, and we can better deal with competing objective functions of the algorithms, such as privacy and prediction quality (Doshi-Velez and Kim, 2017). Interpretation also lets us learn from the model, and convert interpretations and explanations into knowledge (Shrikumar et al., 2016). Moreover, the EU General Data Protection Act (GDPR) provides individuals the right to receive an explanation for algorithmic decisions which significantly affect that individual (Goodman and Flaxman, 2017).

*Corresponding author.

Email addresses: brandseter@gmail.com (Andreas Brandsæter), glad@math.uio.no (Ingrid K. Glad)

1.1. Available methods

One way to achieve interpretability is to use interpretable models, such as linear regression, logistic regression and decision trees. However, one can argue that sufficiently high-dimensional models, for example deep decision trees, can be considered less transparent than comparatively compact neural networks. Several methods have been proposed and developed to interpret the black-box models and explain their predictions. Some of these methods are model-specific, that is, they can only be used on specific machine learning models, while other methods are model-agnostic, and these are the focus of this study. If a task should be solved with machine learning methods, typically, several types of models are evaluated. The use of model-agnostic explanation methods allows us to compare different models in terms of interpretability (Molnar, 2019, Ch. 5).

1.1.1. Feature importance

One frequently used approach to interpret and explain the decisions and predictions made by machine learning algorithms is the concept of feature importance. For a linear regression model, the importance of different features is readily available, and various methods aim to provide a similar interpretation of more complex models. A feature's relative importance can for example be estimated by perturbing the values of the test point, and observing and analysing how the prediction changes (Breiman, 2001; Fisher et al., 2018). Another approach is to approximate the black-box model with an interpretable surrogate model, and base the explanation on the surrogate. Ribeiro et al. (2016) propose a local surrogate method, LIME, which approximates any machine learning model locally with an interpretable model (for example a linear model), and use this model to explain individual predictions. Another popular estimate of local feature importance is the so called Shapley value. The Shapley value concept originates from coalitional game theory, developed to fairly distribute the payout among a set of cooperating players. A prediction is explained by treating the features as players in a game where the prediction is the payout. We describe the Shapley value in more detail in Section 2.

1.1.2. Case-based explanations

Feature importance constitutes an important aspect when predictions using machine learning methods are to be explained and interpreted. However, since the predictions made by the data-driven methods rely heavily on the training data used, we also advocate explanations which convey how the training data affects the predictions.

Case-based (also called example-based) explanations are sometimes useful. One of the simplest case-based learning methods is nearest neighbour models. A k -nearest neighbour model finds the k observations in the training set whose input features are most similar to the input features of the test point, and returns as a prediction for that

test point the outcome from the most similar observations in the training data.

In general, case-based explanation methods work well if the feature values of a specific data point carry some context, meaning the data has a structure, like images or texts (Molnar, 2019, Ch. 5). The case-based explanation methods select particular observations of the dataset to explain the behaviour of machine learning models.

Caruana et al. (1999) proposed a method to generate similar case-based explanations for non-case-based learning methods, claiming it to be very useful especially in medical applications, since medical training and practice emphasize case evaluation.

1.1.3. Influential statistics and influence functions

Koh and Liang (2017) suggest that we can better understand a model's behaviour by studying how the model is derived from its training data, and propose to identify training points most responsible for a given prediction. When performing classical regression analysis, the influence of specific data points in the training data are commonly estimated using Cook's distance (Cook, 1977). Characteristics of observations which cause them to be influential, again in a classical setting, are investigated in Cook (1979), demonstrating how deleting an observation can substantially alter an analysis.

However, for complex machine learning models trained on large datasets, perturbing the data and retraining the model for each point in the training data can be prohibitively expensive. To overcome this challenge, Koh and Liang (2017) use influence functions which tell us how the model parameters change when a point in the training dataset is up-weighted by an infinitesimal amount.

1.2. Training data subset importance

The influence measures only take into account the influence of individual data points. Larger groups of points may together strongly influence the model training and hence prediction. For example, for many machine learning models, if two points in the training dataset are duplicates, removing one of them will not influence the model, while removing both will significantly change the model. For example, for a k -nearest neighbour model, if we have $k + l$ identical points, removing l of them will not change predictions.

Unfortunately, if we try to systematically delete combinations of points from the training data, the number of possible combinations explodes. A quantification of the importance of each of the points in the full training data is also difficult to interpret due to the large size of the data. Therefore, in this paper, we rather concentrate on the importance of different predefined *subsets* of the training data, and propose to explain individual predictions by quantifying how different subsets of the training data affect the predictions. Koh and Liang (2017) encourage this idea, suggesting that sometimes we might be interested in

broader effects, rather than from individual observations, such as for example how a subpopulation of patients from a specific hospital affects a fitted model.

Koh and Liang (2017) argue that since influence functions depend on the model not changing too much, how to analyse the effect and importance of subsets of the training data is an open problem. We propose to use Shapley values to approximate the importance of the different subsets to quantify how the training data affects the predictions. When Shapley values are used to calculate and estimate feature importance, the features act as players in a game where the predictions are the payouts. In our proposed methodology, the subsets replace the features as players. Hence, we call the new measure the Shapley value for training data subset importance.

The case based explanations described in Section 1.1.2 work well when the feature values carry context. Similarly, when the subsets carry context, and the training data can be divided into subsets based on some inherent structure, we believe our proposed explanations provide valuable information.

1.3. Structure of the paper

In the following, we first present the theoretical background for Shapley values of a coalitional game, including its extension to feature importance. Based on this, we explain how we calculate Shapley values for training data subset importance. In Section 3, we demonstrate the methodology and its capabilities. We discuss challenges and limitations in Section 4, and conclude in Section 5.

2. Methodology

2.1. Shapley values of a coalitional game

A coalitional game $\langle N, v \rangle$ consists of a finite set of players N , and a value function $v : 2^{|N|} \rightarrow \mathbb{R}$ which maps a coalition $S \subseteq N$ of players to the real numbers, such that $v(\emptyset) = 0$. N denotes the *grand coalition* of all players. We also assume that the players not belonging to a coalition S do not have any influence on $v(S)$. The value function $v(S)$ describes how much collective payout a set of players can gain by forming the coalition S .

A *solution* of a game $\langle N, v \rangle$ is a mapping that assigns to each player her expected marginal contribution, that is splitting the worth of $v(N)$ among the players in a "fair" way. In general, the marginal contribution of a player depends on the order in which she joins the coalition (Çetiner, 2013). Depending on how we define "fair", different solution concepts are preferred. Çetiner (2013) provides good explanations to most common concepts, including *the Core* and variants of this, *the Nucleolus*, *the Kernel*, the *Owen set* and *the Shapley value*. In this paper, we devote our attention to the latter solution. The Shapley value was introduced by Shapley (1953), and it has a set of desirable properties as we will see below.

Shapley (1953) expresses the Shapley value of player i in a coalitional game $\langle N, v \rangle$ as

$$\varphi_i = \sum_{S \subseteq N \setminus \{i\}} \frac{|S|!(|N| - |S| - 1)!}{|N|!} \cdot [v(S \cup \{i\}) - v(S)] \quad (1)$$

where $|N|$ is the total number of players, $|S|$ denotes the number of players in coalition S , and $v(S)$ describes the total expected sum of payouts the members of S can obtain by cooperation. The sum extends over all subsets S of $N \setminus \{i\}$. We also define the non-distributed gain $\varphi_0 = v(\emptyset)$, which describes the fixed payoff which is not associated to the actions of any of the players, although this is often zero for coalitional games (Aas et al., 2019).

The Shapley value of a player is the average of its marginal contributions with respect to all the permutations. Hence, an alternative expression of the Shapley value of player i in a coalitional game $\langle N, v \rangle$ is

$$\varphi_i = \frac{1}{|N|!} \sum_{\mathcal{O} \in \pi(|N|)} [v(\text{Pre}^i(\mathcal{O}) \cup \{i\}) - v(\text{Pre}^i(\mathcal{O}))], \quad (2)$$

where $\pi(|N|)$ is the set of all permutations of $|N|$ elements, and $\text{Pre}^i(\mathcal{O})$ is the set of all players which precede the i -th player in permutation $\mathcal{O} \in \pi(|N|)$. For more details, see Çetiner (2013), Castro et al. (2009) and Štrumbelj and Kononenko (2011).

Shapley (1953) shows that the Shapley value is the unique solution which satisfies the following properties:

Efficiency: The total gain is distributed:

$$\sum_{i=0}^{|N|} \varphi_i = v(N) \quad (3)$$

Symmetry: If i and j are two actors who are equivalent in the sense that

$$v(S \cup \{i\}) = v(S \cup \{j\}) \quad (4)$$

for every subset S of N which contains neither i nor j , then $\varphi_i = \varphi_j$.

Linearity: If two coalitional games described by gain functions v and w are combined, then the distributed gains should correspond to the gains derived from v and the gains derived from w :

$$\varphi_i(v + w) = \varphi_i(v) + \varphi_i(w) \quad (5)$$

for every $i \in N$. Also, for any real number a

$$\varphi_i(av) = a\varphi_i(v) \quad (6)$$

for every $i \in N$.

Zero player (null player): $\varphi_i = 0$ if player i is a null-player. A player is null-player if she does neither good nor bad to any coalition, i.e. $v(\{i\}) = 0$ and $v(S \cup \{i\}) = v(S)$ for all coalitions $S \in N$.

In the following, we show how we can let features and subsets of the training data act as players.

2.2. Shapley values for feature importance

Lipovetsky and Conklin (2001) apply Shapley values to determine the comparative usefulness of features/regressors in multiple regression analysis, specifically focusing on the difficulties due to multicollinearity among features. Shapley values are also applied by Štrumbelj and Kononenko (2010) to quantify the comparative importance of features, with focus on explaining individual predictions produced by classification models. They propose a *sampling-based* method to approximate the Shapley values to overcome the initial exponential time complexity. Štrumbelj and Kononenko (2011) adapt the explanation method for use with regression models. Lundberg and Lee (2017) propose an alternative approximation method called the *Kernel SHAP*. According to the authors, this method can improve the sample efficiency of the model-agnostic estimators by restricting attention to specific model types, and develop faster model-specific approximation methods. Aas et al. (2019) extend the *Kernel SHAP* method to handle dependent features.

In the following we briefly review the *sampling-based* explanation method proposed by Štrumbelj and Kononenko (2011), to efficiently calculate the Shapley value for feature importance in a regression model. We refer to Štrumbelj and Kononenko (2010, 2011) and Lipovetsky and Conklin (2001) for more details.

We consider a standard machine learning setting where a training set \mathcal{D}^{train} , consisting of J -dimensional feature vectors and corresponding observed responses, is used to train a predictive model f . Let the feature space be defined as $\mathcal{A} \in \mathcal{A}_1 \times \mathcal{A}_2 \times \cdots \times \mathcal{A}_J$, and let p be the probability mass function defined on \mathcal{A} . Here, we assume that individual features are mutually independent. For the dependent case, see Aas et al. (2019). Now let the features in such a model act as players in the game defined in Section 2.1. The aim is to express how each feature affects the prediction of a model $f : \mathcal{A} \rightarrow \mathbb{R}$ in a specific test data point $x \in \mathcal{A}$. Let the contribution of a subset of feature values in this specific data point be the expectation caused by observing those feature values. Formally, the value function is given as

$$v(S)(x) = \sum_{z \in \mathcal{A}} p(z) (f(\tau(x, z, S)) - f(z)), \quad (7)$$

where $\tau(x, z, S) = (u_1, \dots, u_J)$ such that $u_j = x_j$ iff $j \in S$ and $u_j = z_j$ otherwise. The x values are the true explanatory variables of the investigated data point, while z are random data points from the feature space \mathcal{A} . For simplicity, assume that \mathcal{A} is discrete. In the continuous case, the second sum in the following expression is replaced by an integral. The Shapley value (2) for the j -th feature of the game $\langle N, v \rangle$, with v defined in (7), is now

$$\begin{aligned} \varphi_j(x) = & \frac{1}{J!} \sum_{\mathcal{O} \in \pi(J)} \sum_{z \in \mathcal{A}} p(z) \cdot \\ & \left[f(\tau(x, z, \text{Pre}^j(\mathcal{O}) \cup \{j\})) - f(\tau(x, z, \text{Pre}^j(\mathcal{O}))) \right], \end{aligned} \quad (8)$$

where $\pi(J)$ is the set of all permutations of the J different features, and $\text{Pre}^j(\mathcal{O})$ is the set of all features which precede the j -th feature in permutation $\mathcal{O} \in \pi(J)$. Note that the term $f(z)$ occurs for both $v(\text{Pre}^j(\mathcal{O} \cup \{j\}))$ and $v(\text{Pre}^j(\mathcal{O}))$, hence they cancel.

To calculate an exact Shapley value, all possible coalitions have to be evaluated with and without the j -th feature. Since we do not know the distribution $p(z)$, computing $v(S)$ is difficult. Furthermore, the number of possible coalitions of a set N of $|N|$ features is $2^{|N|}$. Hence, finding the exact solution becomes impossible, except with very few features. However, the Shapley values in the form presented in (8) facilitate the use of random sampling and an efficient approximation algorithm. See Castro et al. (2009) and Štrumbelj and Kononenko (2010, 2011) for details. The approximated Shapley value for feature importance is given as

$$\hat{\varphi}_j(x) = \frac{1}{M} \sum_{m=1}^M \left[f(\tau(x, z^m, \text{Pre}^j(\mathcal{O}^m \cup \{j\}))) - f(\tau(x, z^m, \text{Pre}^j(\mathcal{O}^m))) \right], \quad (9)$$

where for each sample m , a permutation $\mathcal{O} \in \pi(|N|)$ and a point $z^m \in \mathcal{A}$ are sampled according to p . Since p is usually unknown, in practice this means resampling from a dataset, as described by Štrumbelj and Kononenko (2010, 2011). In this way, $\hat{\varphi}_j(x)$ approximates how the prediction of the data point of interest, x , depends on the j -th feature.

2.3. Shapley values for subset importance

To understand and interpret how a model produces a prediction for a specific data point, the above Shapley value for feature importance is a useful measure. In addition to such feature importance, it is essential to understand the data used to train the model, and to understand how the data affects the model's predictions. We propose to obtain a measure of the importance of the various subsets of the training data, by letting the different subsets of the data take part as players in a game where the predictions are the payouts.

As in the previous section, we consider a regression function $f : \mathcal{A} \rightarrow \mathbb{R}$, where $\mathcal{A} \in \mathcal{A}_1 \times \cdots \times \mathcal{A}_J$. Now, we divide the training dataset into K disjoint subsets Q_k , such that $Q_1 \cup \cdots \cup Q_K$ is equal to the full training dataset \mathcal{D}^{train} . We let the different subsets Q_k be the players in the game $\langle N, v \rangle$. As before, we let N be the grand coalition, which means that N is the dataset which contains

all subsets, and hence $N = \mathcal{D}^{train}$. We let $S \subseteq N$ denote coalitions of subsets of the training data.

The aim is to investigate how the learning process of the model is affected by the different subsets of the training data. That is, for a new data point $x \in \mathcal{A}$, we are interested in how the data in subset Q_k contributes to the prediction of $f(x)$. Hence, we define the game $\langle N, v \rangle$ with value function

$$v(S)(x) = f_S(x), \quad (10)$$

where f_S is a function which is trained on a dataset composed by the union of Q_k for $k \in S$. We suggest to let the Shapley value for the k -th subset of the game $\langle N, v \rangle$ with value function defined in (10) expressed on the form (2) be

$$\varphi_k(x) = \frac{1}{K!} \sum_{\mathcal{O} \in \pi(K)} \left(f_{\text{Pre}^k(\mathcal{O}) \cup \{k\}}(x) - f_{\text{Pre}^k(\mathcal{O})}(x) \right), \quad (11)$$

where $\pi(K)$ is the set of all permutations of K subsets, and $\text{Pre}^k(\mathcal{O})$ is the set of all subsets which precede the k -th subset in permutation $\mathcal{O} \in \pi(K)$.

When we have no data, that is when $S = \emptyset$, we usually define the predictions to be 0, that is $f_\emptyset(x) = 0$ for all $x \in \mathcal{A}$. This also ensures that $v(\emptyset) = 0$. We interpret the Shapley value of the k -th subset, φ_k , as how much the k -th subset contributes to increase or decrease the prediction relative to 0. In most cases, we find this interpretation most intuitive. However, in cases where we have prior knowledge about the distribution of the response y , it might be beneficial to set f_\emptyset equal to the mean, say, of that distribution. Alternatively, we can pre-process the training data, and center it at 0.

Following the same arguments as for the approximation of the Shapley value for feature importance, a sampling based approximation of the Shapley value for subset importance is

$$\hat{\varphi}_k(x) = \frac{1}{M} \sum_{m=1}^M \left(f_{\text{Pre}^k(\mathcal{O}^m) \cup \{k\}}(x) - f_{\text{Pre}^k(\mathcal{O}^m)}(x) \right), \quad (12)$$

where for each sample m , a permutation $\mathcal{O}^m \in \pi(K)$ is randomly drawn (uniformly).

Other approximations could be suggested, and the statistical properties should be studied and compared. We proceed with (12) in this paper, and show empirically in the Appendix that approximation (12) works well in a small example where it is possible to compute (11) exactly.

The implementation is described in Algorithm 1.

2.4. Shapley values for a performance metric

Various metrics are used to measure the performance or predictive power of a regression model, including absolute error and squared error. Both the value functions

Algorithm 1: Approximated Shapley value for the importance of subset k for data point x .

Required:
Number of iterations M ;
Initialization:
Divide training data into subsets: Q_1, Q_2, \dots, Q_K ;
 $\varphi_k(x) := 0$;
for $m = 1, \dots, M$ **do**
 Sample a random permutation $\mathcal{O} \in \pi(K)$;
 Form dataset \mathcal{D}^+ consisting of Q_k and Q_i for i which precede k in \mathcal{O} ;
 Use dataset \mathcal{D}^+ to train a function $f_{\mathcal{D}^+}$;
 Form dataset \mathcal{D}^- consisting of Q_i for i which precede k in \mathcal{O} ;
 Use dataset \mathcal{D}^- to train a function $f_{\mathcal{D}^-}$;
 Update Shapley values:
 $\varphi_k(x) := \varphi_k(x) + f_{\mathcal{D}^+}(x) - f_{\mathcal{D}^-}(x)$
end
 $\varphi_k(x) := \frac{\varphi_k(x)}{M}$;

(games) presented in (7) and (10) can be modified to one of these performance metrics. The Shapley value of such a game measures the importance of the j -th feature or k -th subset for that performance indicator. In the following, we concentrate on explaining the squared error.

2.4.1. Individual Explanations

We calculate the squared difference between the observed response and the predicted response, and define a game with a value function which compares this with the squared observed response. We denote this game

$$v(S)(x) = (y - f_S(x))^2 - y^2. \quad (13)$$

Since we subtract by y^2 , we ensure that the value function $v(\emptyset) = 0$, since $f_\emptyset(x) = 0$ as defined above.

The Shapley value for subset importance of the k -th subset of this game is given as

$$\varphi_k(x) = \frac{1}{K!} \sum_{\mathcal{O} \in \pi(K)} \left[\left(y - f_{\text{Pre}^k(\mathcal{O}) \cup \{k\}}(x) \right)^2 - \left(y - f_{\text{Pre}^k(\mathcal{O})}(x) \right)^2 \right], \quad (14)$$

where $\pi(K)$ is the set of all permutations of K subsets, and $\text{Pre}^k(\mathcal{O})$ is the set of all subsets which precede the k -th subset in permutation $\mathcal{O} \in \pi(K)$. Note that y^2 is present in both $v(\text{Pre}^k(\mathcal{O}) \cup \{k\})$ and $v(\text{Pre}^k(\mathcal{O}))$, and hence they cancel. Whenever $\text{Pre}^k(\mathcal{O}) = \emptyset$, then $f_{\text{Pre}^k(\mathcal{O}) \cup \{k\}} = f_{Q_k}$ and $f_{\text{Pre}^k(\mathcal{O})} = f_\emptyset = 0$.

2.4.2. Global Explanations

We can also define games which consider the global performance, that is the performance on a test dataset \mathcal{D}^{test} .

We can for example define the game which corresponds to the mean squared error (*MSE*), that is

$$\bar{v}(S)(x) = \frac{1}{T} \sum_{t=1}^T \left[(y_t - f_S(x_t))^2 - y_t^2 \right], \quad (15)$$

where T is the number of points in the test dataset \mathcal{D}^{test} .

Proposition 1. *The global Shapley value for the mean squared error game (15) is equal to the mean of the individual Shapley values for the squared error game (13).*

PROOF. The global Shapley value $\bar{\varphi}_k$ of the k -th subset of the game (15) is given as

$$\begin{aligned} \bar{\varphi}_k &= \frac{1}{K!} \sum_{\mathcal{O} \in \pi(K)} \left[\frac{1}{T} \sum_{t=1}^T \left(y_t - f_{\text{Pre}^k(\mathcal{O}) \cup \{k\}}(x_t) \right)^2 - \right. \\ &\quad \left. \frac{1}{T} \sum_{t=1}^T \left(y_t - f_{\text{Pre}^k(\mathcal{O})}(x_t) \right)^2 \right] \\ &= \frac{1}{T} \sum_{t=1}^T \frac{1}{K!} \sum_{\mathcal{O} \in \pi(K)} \left[\left(y_t - f_{\text{Pre}^k(\mathcal{O}) \cup \{k\}}(x_t) \right)^2 - \right. \\ &\quad \left. \left(y_t - f_{\text{Pre}^k(\mathcal{O})}(x_t) \right)^2 \right] \quad (16) \\ &= \frac{1}{T} \sum_{t=1}^T \varphi_k(v)(x_t), \end{aligned}$$

where we omit y_t^2 since they occur in both $v(\text{Pre}^k(\mathcal{O}) \cup \{k\})$ and $v(\text{Pre}^k(\mathcal{O}))$, and hence cancel.

2.5. Computational effort

When approximating the Shapley values (12), the model is retrained for each sample $m \in \{1, \dots, M\}$. This also applies to tuning of hyper-parameters. However, the effort is usually significantly smaller than training the original model, because the size of the various datasets, which depends on the size of the coalition $S^m \subseteq N$, is significantly reduced for many of the samples. Nevertheless, the method is computationally expensive. Fortunately, the re-training can be done in parallel. Furthermore, the re-training process does not need to be performed repeatedly for each new test point $x \in \mathcal{D}^{test}$. When a model is trained, it can be reused when explaining a new prediction. Furthermore, in our experience, the Shapley values rapidly converge.

In appendix A, we consider an example where we derive the exact Shapley values for training data subsets, and explain the calculations step by step. We compare the results with the approximated values from the implemented algorithm. We strongly recommend this example to readers who aim to implement the methodology, and pursue a comprehensive overview of the technicalities.

3. Demonstrations and use cases

When time series data is evaluated, the training data can be divided into subsets based on chronological time. For example, when we analyse the classifications made by an autonomous vehicle, subsets can comprise data from specific months. The Shapley values for subset importance reveal how each subset in the training dataset contributes to the prediction. The user can further investigate subsets for which contributions are significantly different from the other subsets. Maybe similar objects are present in these subsets, or these subsets might contain other similarities to the situation in question, such as similar traffic complexity, similar weather conditions, or similar operational mode, etc. Note that the sizes of the subsets do not have to be equal.

We can also invoke the subsets based on a feature of interest. We can for example split the training data into subsets such that each subset only comprises training data instances which, for the feature of interest, lie within a particular range. By combining Shapley values for training data subset importance with feature importance, we can produce more comprehensive explanations. Not only can we explain that a feature is important, but we can also explain how different parts of the training data affect the specific prediction in question.

It is also possible to invoke the subsets based on features or information which are not used by the model. If a feature is omitted when making a prediction, for example to avoid using models which make discriminative decisions, we can still invoke the subsets based on this feature (assuming of course that we do have this information). Furthermore, explanations based on Shapley values for training data subset importance can still be useful in cases where explanations based on feature importance are less informative due to uninformative features.

In the following, we provide a set of examples to illustrate the proposed methodology, and show how we can use the Shapley values for training data subset importance to better understand how the training data affects individual predictions in \mathcal{D}^{test} .

3.1. The Shapley values are as expected when the signal generating function is known

We consider a simple simulated time series regression problem. Let

$$x_j(t) = \sin(\omega_j t) + \eta_j(t), \quad j = 1, \dots, 4 \quad (17)$$

where $t = 1, \dots, N$, $\eta_j(t) \sim N(0, 0.1)$, and ω_j are sampled uniformly from $[2\pi, 40\pi]$. We define a data generating model

$$y(t) = x_1(t) \cdot x_2(t) + x_3(t) \cdot x_4(t) + \epsilon(t), \quad (18)$$

where the x_j -s are explanatory variables, and the noise term $\epsilon(t)$ is iid $N(0, 0.1)$. We simulate data which we use to train a random forest model, with the randomForest

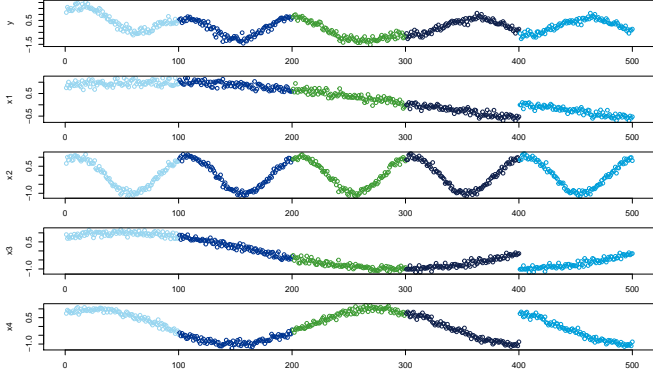


Figure 1: Training dataset used in the simulated time series example. The five different data subsets are marked with different colors.

package (Liaw and Wiener, 2002) in R (R Core Team, 2019). We use a model with 100 trees and set the maximum number of terminal nodes to 30.

When we explain the predictions, we assume that we have no knowledge about the algorithm used to produce the predictions (black-box). To calculate the Shapley values for training data subset importance, we need access to retrain the model, but we do not inspect the algorithm, nor the training data. We assume that the retraining process is fully automated. This includes hyper-parameter optimization if this is performed for the implemented model.

3.1.1. Dataset

We first simulate 400 data points from the model above. We split this training dataset into four subsets, such that each subset contains 100 points. We duplicate the fourth subset, such that the total training dataset comprises 500 data points, and five subsets. We do this both in the training dataset and the test dataset. This allows us to demonstrate the symmetry property; when subsets of the training data are equal, so are the Shapley values.

Due to the subjective and approximate nature of explanations, testing and verifying the quality and trustworthiness of an explanation is difficult. Hall and Gill (2018) suggest to use simulated data with a known signal generating function to test that the explanations accurately represent that known function. Thus, in this example, we let the test data be equal to the training data. This is of course unrealistic in practice, but the aim is to make it easy to understand how the explanations can be used. This also enables us to better validate the quality of the explanations. The dataset is illustrated in Figure 1.

3.1.2. Explaining predictions

Shapley values of five selected observations (marked with red in the upper plot) are provided in Figure 2. In the upper plot of Figure 2, the predicted response is plotted for all points in the test dataset of 500 points, which are equal to the training data shown in Figure 1. The predictions are produced by a model which is trained on the full training dataset which comprises all the subsets,

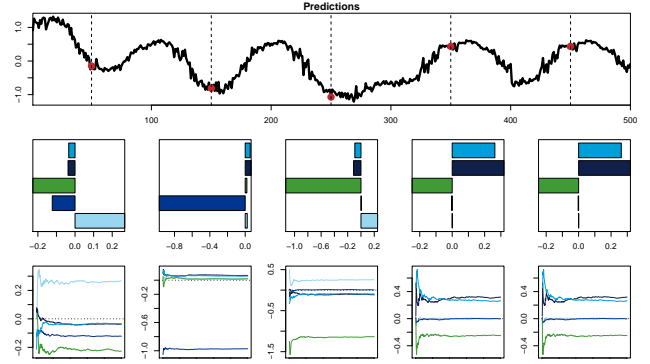


Figure 2: Explanations of selected time points $t = \{50, 150, 250, 350, 450\}$, using Shapley values for subset importance. The five different Shapley values (one for each subset) are marked with different colors as in Figure 1.

that is the predictions are made by the fitted model f_N . Remember that for illustrative purposes, the test dataset is identical to the training dataset. In the middle row of Figure 2, explanations of the five selected instances are shown. The estimated Shapley values for subset importance of the five subsets are plotted. The bars are colored in the corresponding colors. The plots in the bottom row show how the Shapley value estimates develop when the number of samples m is growing from 1 to M . Here, we use $M = 250$.

When interpreting the explanations, the analogy to coalitional game theory is fruitful. The Shapley value of a coalitional game fairly distributes the payouts of a game between the cooperating players. As stated, in our game, the subsets are the players and the predictions are the payouts. Hence, we interpret the Shapley value of a subset, as that subset's contribution to the prediction. For example, if we investigate the first data point we explain, that is at time $t = 50$, we observe that the Shapley values show that the first subset contributes to increase the prediction, while the other four subsets contribute to decrease the prediction. The predictions at the next two data points we explain ($t = 150$ and $t = 250$) are significantly decreased by subset 2 and 3 respectively. Both instances have a true response far below 0. It is also evident that the two last time points, which have identical instances of interest, exhibit approximately the same sets of Shapley values.

3.1.3. Properties

In theory, the two equal subsets (4 and 5) should receive the same Shapley values for all the data instances of interest. This is in accordance with the symmetry property as defined in (4). In Figure 3a, we have plotted the Shapley values of the two subsets for all instances in the test dataset, and we observe that the values are equal, except for sampling variability.

Figure 3b demonstrates that the efficiency property as defined in (3) is satisfied. The upper plot of Figure 3b shows the predictions made by f_N and f_\emptyset , in red and grey color respectively. f_N denotes the model which is trained

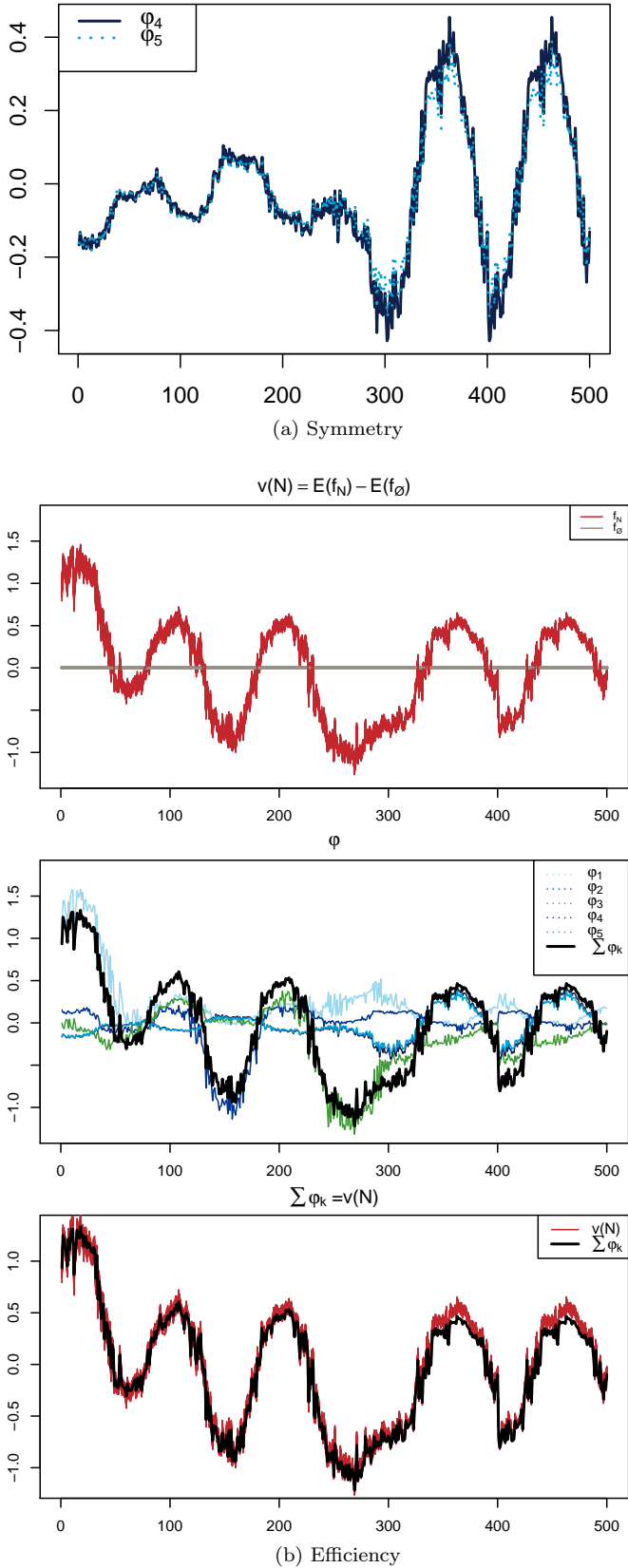


Figure 3: Demonstrates that the symmetry and efficiency properties are satisfied.

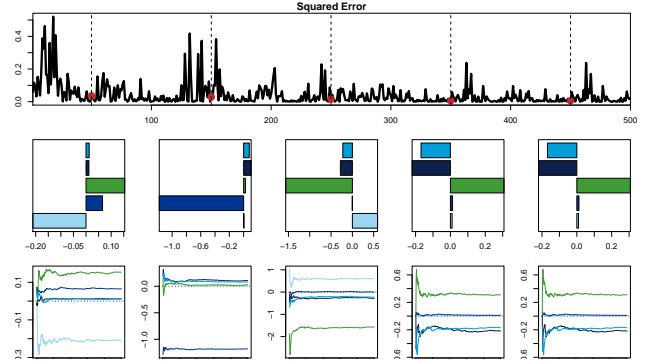


Figure 4: Explanations of data point number $\{50,150,250,350,450\}$, using Shapley values for subset importance for the squared error.

with the full training dataset. When we have no data, we choose to let the predictions be zero, that is $f_\emptyset = 0$. The middle plot shows the Shapley values for each subset, in addition to the sum of the Shapley values. Finally, in the lower plot, the sum of the estimated Shapley values is compared to the estimated total gain, and we observe that they are approximately equal. This means that the total gain is distributed, that is that the sum of the Shapley values, $\sum_{k \in N} \varphi_k(v)$, equals the value of the grand coalition, $v(N)$.

3.1.4. Explanations of Squared Error

In Figure 2, the actual predictions in five selected points are explained, and the Shapley values show how the different subsets contribute to increase or decrease the predictions. This corresponds to the game presented in (10). Figure 4 provides explanations related to the squared prediction error, as described in the game presented in (13). Here, the Shapley values show how the different subsets contribute to decrease or increase the squared error in the five chosen instances of interest. This game assumes knowledge of the corresponding observed response, y . Obviously, in practice, the response is often not available, but it can for example be available on a test dataset, used for verification purposes before the model is deployed.

We observe that for each of the explained data points, the Shapley value is negative for the subset it belongs to. The training dataset and test dataset are identical in this example, and hence we expect the squared error to be reduced in these situations. We also observe that the Shapley values of subset 4 and 5 are very similar, which also is as we expected since these subsets are identical. The explanations of the predictions at time $t = 350$ and $t = 450$, show that the third subset of the training data contributes significantly to increase the squared error, and hence decrease the performance. The same effect is evident at time $t = 250$, but now, it is subset 1 which contributes to increase the squared error.

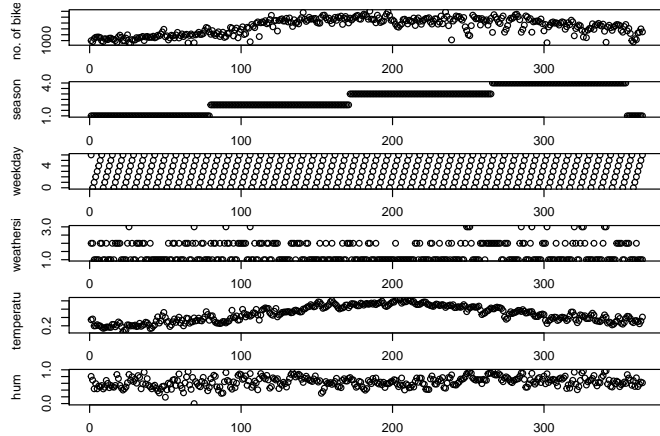


Figure 5: Training dataset used in the bike rental example.

3.2. The explanations of predictions by simple models correspond to the intuitive explanations

We explain a machine learning model which predicts the daily number of rented bikes, based on corresponding weather and seasonal information. The predictions in this example are made using simple and intuitive models which in principle should be easy to interpret. However, we assume that we have no knowledge about the models which are used.

The machine learning model is trained on the Bike Sharing dataset (Fanaee-T and Gama, 2013), which comprise data from year 2011 and 2012 in a capital bike-share system. The training data comprises data from the first year, and we use the second year for testing. The available explanatory variables include weather and seasonal information. For simplicity, we concentrate on a selection of the available explanatory variables, and use the five features listed in Table 1.

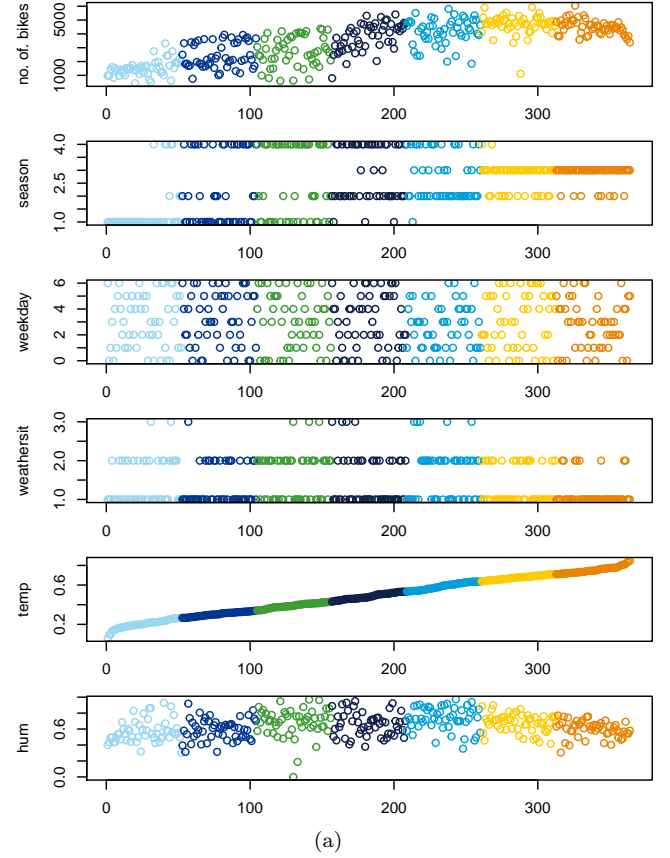
name	description
season	1: winter, 2: spring, 3: summer, 4: fall
weekday	day of the week
weathersit	1: clear/partly clouded, 2: misty, 3: light precipitation, 4: heavy precipitation
temperature	normalized temperature
humidity	normalized humidity

Table 1: Features used to predict the daily count of rented bikes.

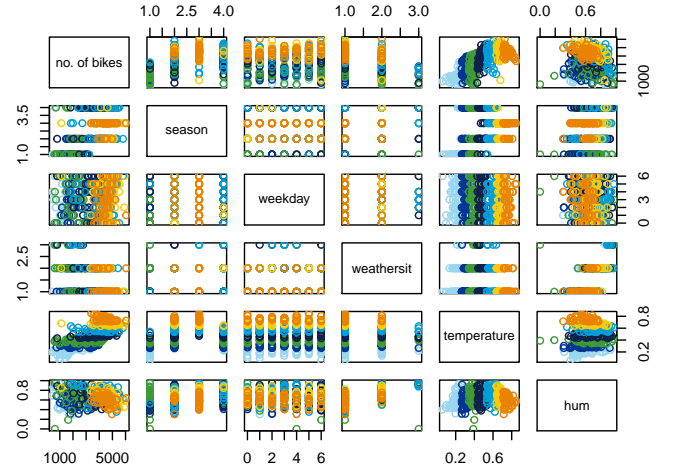
The training data is illustrated in Figure 5. Predictions are produced for the points in the test dataset, and we assume that we are asked to explain the predicted count of rented bikes on four days in the test dataset (year 2): day 46, 137, 228 and 320.

3.2.1. Feature importance

Before we explain the predictions using Shapley values for training data subset importance, we calculate and analyse the Shapley values for feature importance of the four selected days. We use the *iml*-package (Molnar et al.,



(a)



(b)

Figure 6: Training dataset which is split into subsets based on temperature. The data points' membership in the different subsets are indicated with different colors. Figure (a) shows trace plots of each feature. Additionally, the response (the number of rented bikes) is shown on top. Note that the observations are sorted according to temperature, hence the numbers on the horizontal axis do not correspond to the days of the year. In (b), the same data is illustrated with a scatterplotmatrix.

2018) in R (R Core Team, 2019), which computes the Shapley values for feature importance following the methodology by Štrumbelj and Kononenko (2014) as described in Section 2.2. The values are not shown, but not surprisingly, both season and temperature significantly affect the predictions. For example, we observe that for the first and last explained day (day 46 and day 320), the temperature contribute to decrease the predicted number of bike rentals, relative to the mean, while for the two middle days (day 137 and day 228), the temperature contribute the most to increase the predicted number of rented bikes.

3.2.2. Training data subset importance

To approach a deeper understanding of how temperature affects the predictions, we propose to calculate and analyse Shapley values for training data subset importance, and base the subsets on increasing temperature. We choose to use seven different equally sized subsets, ordered by increasing temperature. The subsets of the training data are illustrated in Figure 6a and 6b.

The Shapley values for training data subset importance for the four days of interest are presented in Figure 7. Here we define the non-distributed gain, φ_0 , to be equal to the mean of the response of the training data. Hence, the Shapley values show how the seven different subsets change the predicted number of rented bikes relative to the mean response in the training data. The upper plot shows the predictions for all days in the test dataset which comprises data from year two. The temperature is shown in the second row. The values for the four selected days are marked with red points. The Shapley values for subset importance are shown in the third row, in ascending order (subset 1 at bottom (light blue), and subset 7 at top (orange)). The plots in the bottom row, show how the Shapley value estimates develop when the number of Monte Carlo iterations m is growing from 1 to 250.

In Figure 7, we observe, for the prediction at day 46, that the subsets which comprise the data with highest temperature (subset 6 and 7) contribute significantly to increase the prediction. The same applies to the prediction at day 320. Note that the observed temperature is quite low at these days. The predictions at the two middle days (day 137 and 228), however, are not specifically increased due to training data subsets with the highest temperatures, even though the temperature at the selected days is high. To make it easier for us to assess and evaluate the quality of our explanations, the black-box model used here, is a linear model. Knowing this, and also having a second look at the training data in Figure 6b, we can argue that the explanations above are reasonable. When fitting a linear model, the slope of the model is not necessarily increased by adding training data instances with high response values. For example, the instances in the seventh subset, have both high response values and high temperatures, but if we investigate Figure 6b closely, this subset seems to decrease the slope. Decreasing the slope, leads to lower predictions for instances with high temperature,

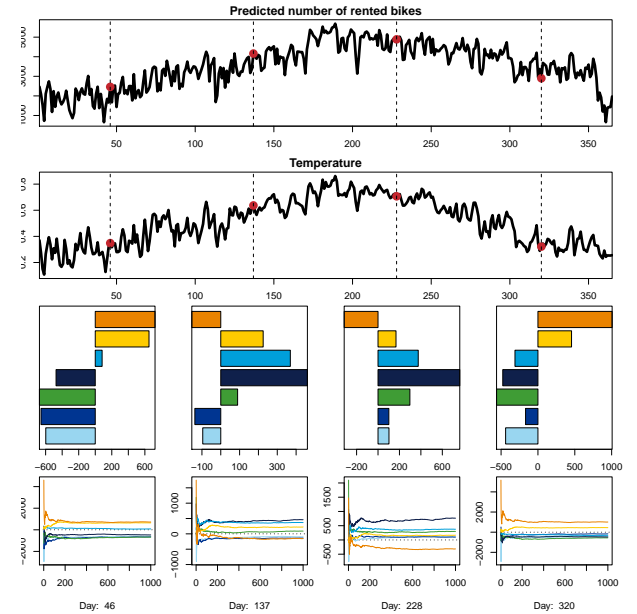


Figure 7: Shapley values for training data subset importance used to explain predictions of a linear regression model on the test dataset (2012). The Shapley values show how the different subset contribute to change the prediction relative to the mean of the response in training data, $\bar{y} = 3405.762$

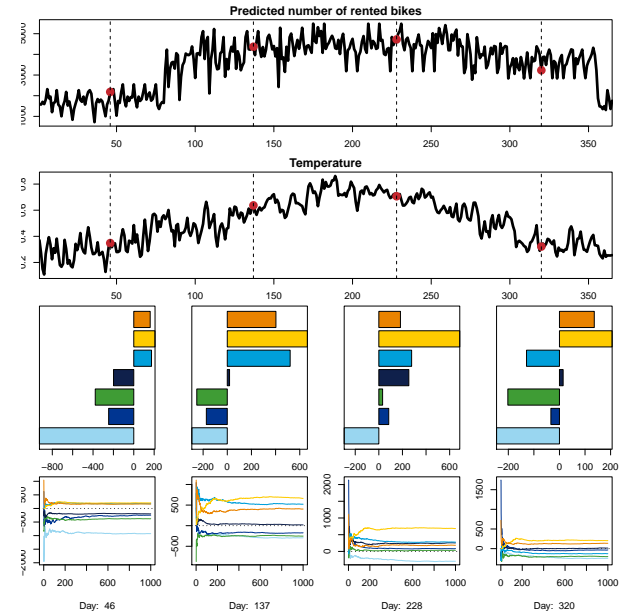


Figure 8: Shapley values for training data subset importance used to explain predictions of a nearest neighbour model with 3 neighbours. The Shapley values show how the different subset contribute to change the prediction relative to the mean of the response in training data, $\bar{y} = 3405.762$

while when the temperature is low, the predictions will be higher.

Suppose now that the linear model is replaced by a nearest neighbour model. The predictions and corresponding explanations are shown in Figure 8. Changing the model, obviously leads to different predictions and explanations. Now, the subsets with high temperature contributes to high predictions, and the subsets with low temperature contributes to low predictions.

Obviously, linear models and nearest neighbour models are in principle easy to interpret, and one can argue that such models do not need any further explanations. Remember that in reality we do not know which models are used and treat the models as black-boxes. The reason for choosing to explain these simple models is to demonstrate that the explanations using Shapley values for training data subset importance correspond to the intuitive explanations.

3.3. Revealing erroneous training data

Here, we demonstrate how we can use Shapley values for subset importance to reveal erroneous training data. Still for the bike-rental example, we select two days in the training data, day 68 and 78, and alter their response values (see Figure 9) to mimic mislabelled or faulty data. To make the illustration clear and easy to read, we choose to use the training dataset (without the erroneous data points) for testing, and make predictions using a nearest neighbour model with one neighbour (1-NN). For comparison, predictions are also made for 14 days for which predictions are not affected by the erroneous data points. Shapley values for subset importance for squared error are calculated for each prediction as shown in Figure 10. Our explanations show that the second subset (blue) contributes to increase the squared error for the two days affected by the error. For the 14 days which predictions are not affected by the erroneous data points, the Shapley values show that the second subset contributes to decrease the squared error.

3.4. Revealing biased behaviour

Recent studies demonstrate that machine learning algorithms can reproduce and amplify biases from the real world (Buolamwini and Gebru, 2018). For example, Angwin et al. (2016) report that a software used across the United States to predict future criminals has racial bias. Similarly, Lum and Isaac (2016) demonstrate that predictive policing of drug crimes, used by law enforcement to try to prevent crime before it occurs, results in increasingly disproportionate policing of historically over-policed communities.

In this section we consider how explanations based on Shapley values for subset importance can be used to analyse and investigate if a model is discriminative. We consider a simulated example where an algorithm determines the size of a loan a customer is granted by a bank. Suppose the customer wants to know if and how her country

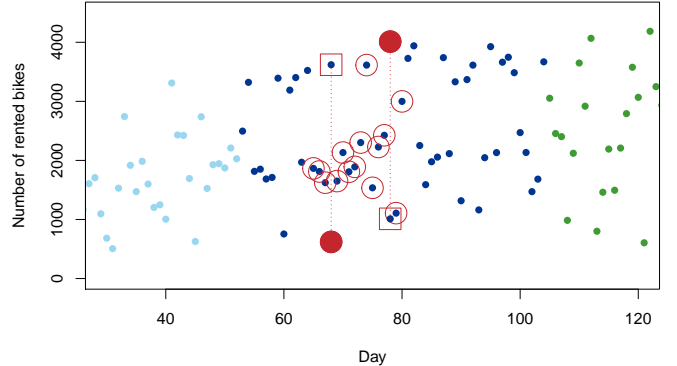


Figure 9: We alter the response on two days in the training dataset to mimic erroneous data points (from red boxes to filled circles). Predictions are also made for 14 days which predictions are not affected by the erroneous data points (red circles).

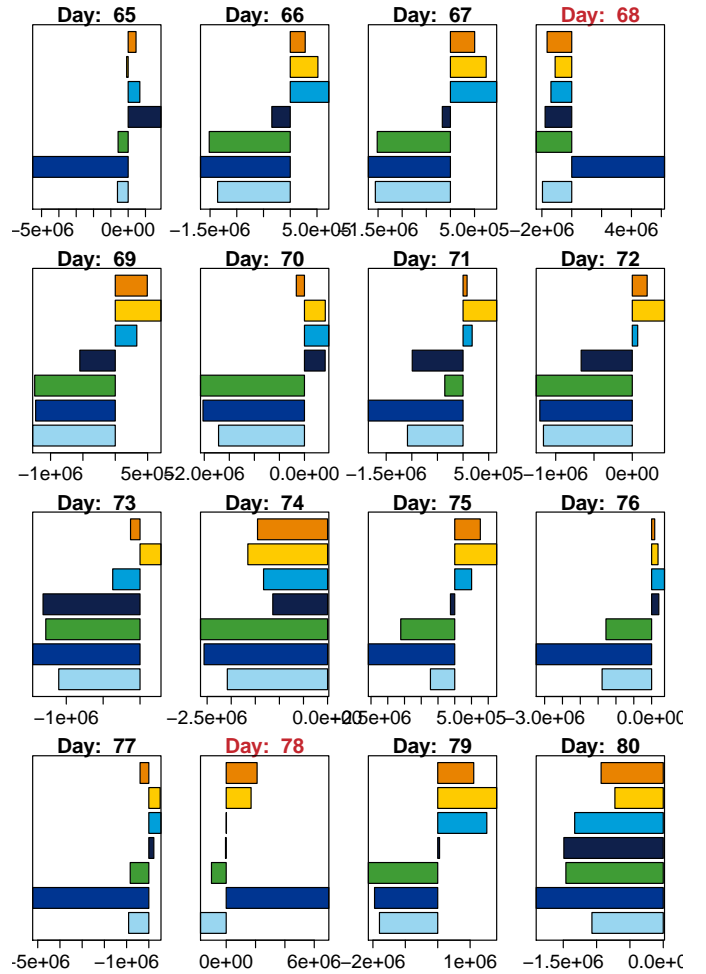


Figure 10: Shapley values for squared error on 16 selected days. Day 68 and 78 (marked with red) are affected by the erroneous data points.

of birth affects the decision. Obviously, if a model uses country of birth as a feature, it is easy to calculate and use the Shapley values for feature importance to explain how this affects the predictions. However, to avoid making the algorithm discriminative, country of birth is typically excluded as a feature. Nevertheless, a prediction can rely on national origin indirectly through other hidden dependencies, such as for example residential area.

Let the size of the granted loan be given by $f : \mathcal{A} \rightarrow \mathbb{R}$, where the feature space $\mathcal{A} \in \mathcal{A}_1 \times \dots \times \mathcal{A}_J$. In addition to the explanatory variables, x_i , for $i = 1, \dots, J$, we define a categorical variable, x_D , which denotes a discriminative property; in this example country of birth. We divide the training dataset into subsets based on x_D , and use Shapley values to quantify the importance of these subsets.

In the numerical results presented below, we divide the test dataset into 3 different subsets (country A , B and C), and let both the training and test datasets comprise 100 instances from each country, such that both the training and test dataset comprise 300 instances in total. Furthermore, we use four explanatory variables ($J = 4$).

3.4.1. Response and explanatory variables independent on the discriminative property

As a baseline, we first define the process generating the response to be white noise, that is

$$y = \epsilon \quad \text{where } \epsilon \sim N(0, 1). \quad (19)$$

Even if the explanatory variables are not involved, we generate x_1, \dots, x_4 also as iid $N(0, 1)$ variables, and use the training dataset with these covariates and this response to train a k nearest neighbour model with $k = 10$.

No matter which model we use, if it is trained on this dataset, it will of course not discriminate based on x_D (country of birth), because both the explanatory variables, x_i , and the response, y , are independent on x_D . Hence, if we explain the predictions for a set of individuals, we expect the average Shapley values for training data subset importance to be approximately zero. We observe this in the three barplots in Figure 11a. Here, the Shapley values for all predictions in a country are calculated, and the average Shapley values for individuals in the *test* dataset belonging to country A , B and C are shown in the upper, middle and lower subplot respectively. The Shapley values for subset importance are shown in light blue, blue and green. These values describe the importance of the three different subsets of the *training* data, comprising individuals from country A , B and C respectively.

3.4.2. Response is dependent on the discriminative property, but explanatory variables are independent

We now change the response in the training dataset such that the response deterministically depends on the sensitive information x_D (country of birth), by letting

$$y = x_D + \epsilon, \quad (20)$$

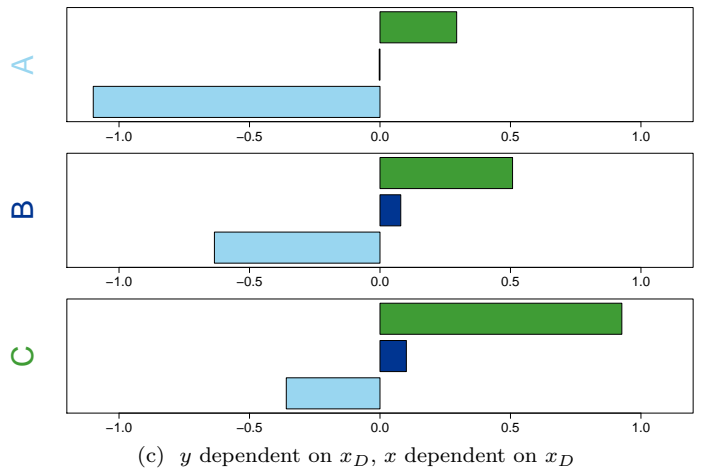
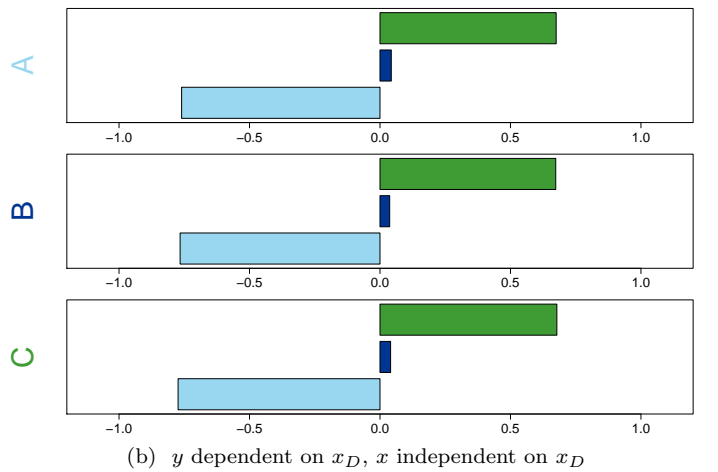
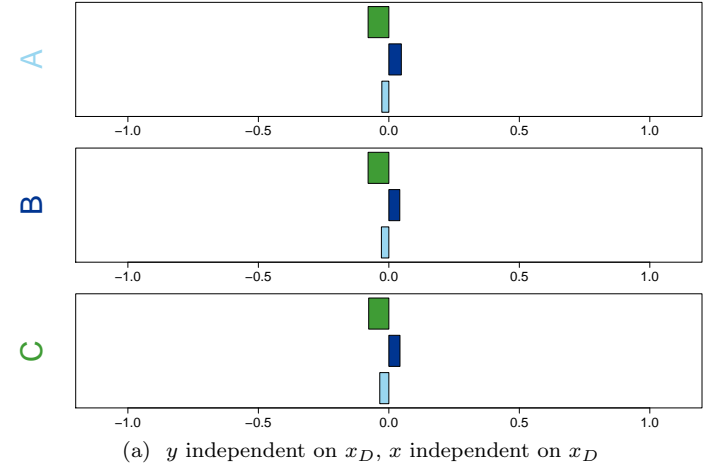


Figure 11: Shapley values for all the test points in a country are calculated, and the average Shapley values for that country is presented. Figure (a), (b) and (c) shows results from calculations described in section 3.4.1, 3.4.2 and 3.4.3 respectively. Results for individuals of the *test* data from country A , B and C are shown in the upper, middle and lower subplots respectively. The Shapley values for training data subset importance of the three countries A , B and C are shown in light blue, blue and green respectively.

where ϵ and x_1, \dots, x_4 are as defined above. We let x_D take values $-1, 0$ and 1 for country A , B and C respectively.

As in Section 3.4.1, we use a k NN model with $k = 10$, now trained on a dataset with the new response values generated by (20). The Shapley values for training data subset importance for the predictions using the new responses are displayed in Figure 11b. The light blue bars show that individuals from country A contribute to decrease the predictions, while individuals from country C contribute to increase predictions. But this does not indicate that the model is discriminative. The explanatory variables x_1, \dots, x_J are drawn from a standard normal distribution, and hence, all the explanatory variables are independent of country of birth (x_D), and therefore the model cannot take country of birth into account. We observe that the three plots are identical, indicating that the individuals in the different groups (A , B and C) are treated equally by the model.

3.4.3. Response and explanatory variables dependent on the discriminative property

However, if we include dependence between x_D and the explanatory variables, the model might be discriminative. In the following, we once again use the response values generated by (20). But now, we alter the explanatory variables x_1, \dots, x_J such that they are dependent on x_D , in the following way

$$\begin{aligned} x_1 &\sim N(x_D, 1) \\ x_2 &\sim N(-x_D, 1) \\ x_3 &\sim N(2x_D, 1) \\ x_4 &\sim N(-2x_D, 1). \end{aligned} \quad (21)$$

The results are displayed in Figure 11c. We observe that predictions for individuals from country A ($x_D = -1$) are severely reduced by individuals from this country (light blue). Individuals from this country also contribute to reduce the predictions of individuals from the other countries, but the reduction is smaller. Similarly, individuals from country C ($x_D = 1$) contribute to increase the predictions of individuals from country C more than individuals from the two other countries. Unlike in Figure 11b, the subsets of the training data now affect individuals from the three countries differently, and this practice can perhaps be regarded as discriminative.

It should be remembered that the discriminative property x_D is not used as a feature in the black-box model and would not have been flagged using standard Shapley values for feature importance.

3.5. Training data selection guided by explanations to improve a predictor

In this section we show how we can use Shapley values for subset importance for squared error to tailor a training data acquisition strategy to improve the accuracy of a

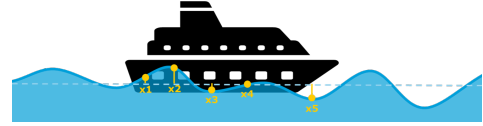


Figure 12: The features we use to predict the vertical bending moment are the undisturbed wave elevations at five different locations along the ship

predictor on a selected subset of interest. This can for example be predictions within a specific range, or as in the following, where we are only interested in predictions in the upper tail of the distribution. We apply the training data acquisition strategy to a real world problem, where a machine learning model is trained to predict the midship vertical bending moments of a ship in operation.

3.5.1. Predicting the vertical bending moment of a ship

We begin by defining the prediction model we wish to improve. The response y is the mid-ship vertical bending moment. The features we use to represent the waves, are the so-called undisturbed wave elevations at five different locations along the ship, see Figure 12. For a detailed description of the prediction model and the underlying dataset, we refer to Oberhagemann et al. (2019). In the following, we treat the prediction model as a black box.

3.5.2. Shapley values based on sea states

Now we divide the training data into subsets based on sea states. A sea state describes the condition of the ocean surface. It is specified by a wave frequency spectrum with a given significant wave height, a characteristic wave period, a mean propagation direction and a directional spreading function (DNV GL, 2017, RP-C205). In applications, the sea state is usually assumed to be a stationary random process. In this study, we disregard the wave direction and spread, and let, for simplicity, significant wave height, H_S (mean wave height of the highest third of the waves), and zero up-crossing period, T_Z (average wave period measured as the time between the successive up-crossings of the mean water level), specify the different sea states.

3.5.3. Improved training data acquisition

Our goal is to construct a training dataset X_{train} , comprising J features, such that the prediction accuracy is increased for the largest vertical bending moments on an unseen test dataset X_{test} , under the assumption that the number of instances in X_{train} is bounded at N . Accurate predictions of the largest bending moments are of great importance in design since these contribute to the extreme wave loads. We assume that we have some knowledge about the data before we start acquiring training data. Specifically, we assume that we have an initial dataset, Z , which we can use to decide a strategy for how we should acquire training data. We split Z into a training and a test dataset, Z_{train} and Z_{test} .

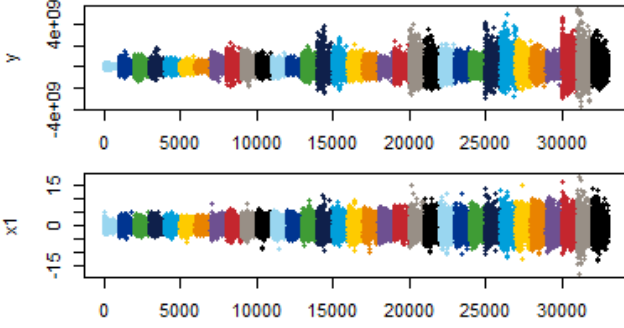


Figure 13: Initial dataset Z_{test} . The top plot shows the true vertical bending moment. The corresponding explanatory variable x_1 is shown in the bottom plot. Plotting the other explanatory variables, x_2, \dots, x_5 , provides a similar pattern, hence these are not shown here. The colors indicate from which sea state the observations originates.

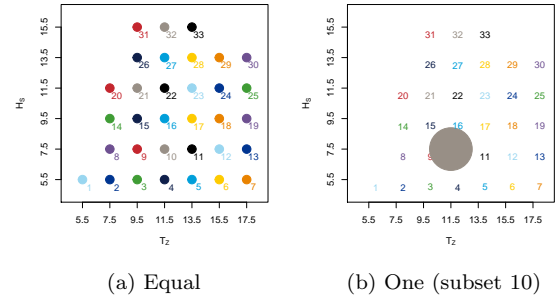
Multiple strategies can be suggested for the above mentioned problem. In the following, we present three different strategies, *equal*, *one* and *max*, where the latter is our proposed strategy, which uses Shapley values, and the first two are presented as baselines:

- *equal* - equally many datapoints are sampled from each sea state,
- *one* - the training dataset comprises all its data from the sea state which the predicted instance originates from,
- *max* - the training data, X_{train} , is sampled from different sea states, proportionally to the average Shapley values of subset importance. The average Shapley values are based on the L largest predictions of the initial test dataset, Z_{test} .

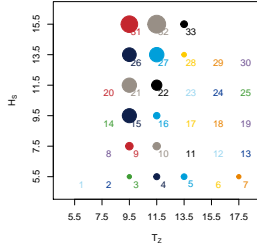
3.5.4. Simulation set-up

The initial test dataset Z_{test} is illustrated in Figure 13. Data from the different sea states are marked with different colors. The dataset comprises sampled data points from 30 minutes simulation in each sea state. We consider a collection of 33 different sea states. In the *max* strategy, we calculate Shapley values for subset importance for prediction accuracy for approximately 3% of the predictions ($L = 1000$); those with the highest predicted bending moment. The training data X_{train} comprise $N = 10000$ instances, regardless of the acquisition strategy.

The number of samples originating from the different sea states for the three different strategies are visualized in Figure 14. The diameter of the circles is determined by the square root of the number of points. For the *equal* and *max* strategy the sampling is identical for each prediction, while for the *one* strategy, all points are sampled from the same sea state for which the predicted instance originates. This means that K different models are fitted, and when we predict the vertical bending moment of an instance which originates from sea state k , the model which is trained on data from sea state k is used.



(a) Equal (b) One (subset 10)



(c) Max

Figure 14: Illustrates the number of instances per sea state in the improved training dataset X_{train} . The size of the circles is determined by the square root of the number of points.

Strategy	rf	10-NN
<i>Equal</i>	1.00	1.00
<i>One</i>	1.02	1.16
<i>Max</i>	0.74	0.67

Table 2: The relative Mean Squared Error of the predictions of the extreme bending moments using three different re-sampling strategies (*equal*, *one* and *max*), and two different models (random forest (rf) and nearest neighbour with 10 neighbours(10-NN)).

3.5.5. Results

Now we apply the prediction models which are trained on datasets generated with the sampling strategies presented above. The test dataset contains 25 780 instances, and these instances are collected from extreme events, collected over simulations corresponding to 50 years of operation in the North Atlantic wave climate, where the duration of each sea state is found according to the North Atlantic scatter diagram (DNV GL, 2017, RP-C205).

We calculate the mean squared error, and present results relative to the *equal* strategy in Table 2. The results are based on 3 300 extreme predictions (100 most extreme predictions from each of the 33 sea states). Predictions are made with two different models; a random forest regressor with 100 trees where the maximum number of terminal nodes is set to 15, and a nearest neighbour model with $k = 10$. The procedure is repeated 100 times, and average results are presented.

We observe that the proposed strategy using subset importance significantly reduced the mean square error com-

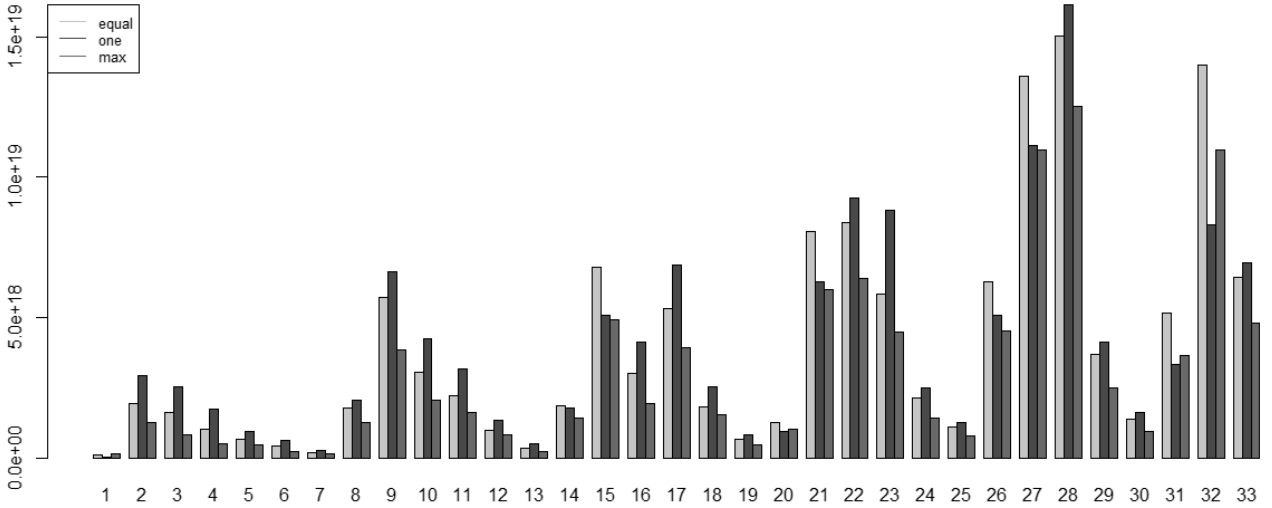


Figure 15: Mean squared error for predictions from 33 specific sea states. Predictions are made with random forest models, trained on datasets which are acquired following the three different data acquisition strategies: *equal*, *one* and *max*.

pared to the two baseline data acquisition approaches. Significant reductions are obtained using both the the random forest regression model and the nearest neighbour model.

Results per subset, using the random forest model, are presented in Figure 15. (To save space, we omit a similar figure displaying results for each sea state using the nearest neighbour model). We observe that in most sea states, the mean squared error is lower for the *max* strategy than for the two other data selection strategies, *equal* and *one*. However, some exceptions can be seen, most importantly for sea state 32, where the *one* strategy outperforms our suggested approach. Nevertheless, in general our approach demonstrates significant improvement. This indicates that the explanations provided by the Shapley value for subset importance are in accordance with the intuitive expectation; that the most important subsets contribute the most to reduce prediction error.

4. Discussion and extensions

4.1. Human subject evaluation

This paper introduces the Shapley values for subset importance, and demonstrates its capabilities on several examples. However, human subject evaluation should in the future be performed to evaluate to what extent humans, both experts and lay users, can make use of the Shapley values for subset importance in practice to increase their understanding and insight about the black-box model.

4.2. Extension to classification

Extension from the regression settings to classification settings is straightforward. In this paper we concentrate on regression problems to ease understanding and notation.

4.3. Combined Shapley values for feature and subset importance

It is possible to construct a combined Shapley value for training data subset and feature importance. To evaluate the importance of a feature j of a regression function $f : \mathcal{A} \rightarrow \mathbb{R}$, and at the same time, the importance of the training data in a subset k , we define a value function $v(S, W)$ which is the expectation of f when it has seen $x \in \mathcal{A}$ for the features in subset $S \subseteq \{\mathcal{A}_1, \dots, \mathcal{A}_J\}$, and f is trained on a dataset composed by the union of subsets Q_k for $k \in S \subseteq \{1, \dots, K\}$.

We define the Shapley value of feature j and subset k by combining (8) and (11),

$$\begin{aligned} \varphi_{jk}(x) = & \frac{1}{K!} \frac{1}{J!} \sum_{\mathcal{B} \in \pi(K)} \sum_{\mathcal{O} \in \pi(J)} \sum_{z \in \mathcal{A}} \\ & p(z) \cdot \left[f_{\text{Pre}^k(\mathcal{B}) \cup \{k\}}(\tau(x, z, \text{Pre}^j(\mathcal{O}) \cup \{j\})) - \right. \\ & \left. f_{\text{Pre}^k(\mathcal{B})}(\tau(x, z, \text{Pre}^j(\mathcal{O}))) \right], \end{aligned} \quad (22)$$

where $\pi(K)$ is the set of all permutations of K subsets, and $\text{Pre}^k(\mathcal{O})$ is the set of all subsets which precede the k -th subset in permutation $\mathcal{O} \in \pi(K)$. Furthermore, $\pi(J)$ is the set of all permutations of the J different features, and $\text{Pre}^j(\mathcal{O})$ is the set of all features which precede the j -th feature in permutation $\mathcal{O} \in \pi(J)$.

Approximation of (22) can be accomplished with simulations following the procedure we described in Section 2.2 to approximate the Shapley value for feature importance.

A further study of the combined Shapley value for feature and subset importance, including interpretation and application, should be a topic for future work.

4.4. Alternative formulation using random values

In this paper, we calculate the Shapley values for training data subset importance by comparing the predictions f_S of a function which is trained on a subset S of the available training data, with the predictions $f_{S \cup \{k\}}$, which is trained on a dataset which in addition comprise the data of subset k . This approach is in line with existing work on influence functions (Koh and Liang, 2017). An alternative formulation is to let f_S be trained on a dataset which consists of the full training dataset, but where the rows which correspond to the data points not comprised in a subset $k \in S$ are replaced by random values inspired by the traditional approach to calculate Shapley values for feature importance. A practical issue arises concerning how to sample both response and features randomly. We have implemented and investigated one version of this alternative formulation, and in the examples we have encountered, the two approaches produce similar explanations. We encourage further investigation of this.

4.5. Subsets based on multiple variables

In this paper we have presented examples where the training data are divided into subsets based on a single feature, such as time, temperature, sea state, etc. It is possible to divide the subsets using multiple variables, and apply different clustering techniques when dividing the data into subsets. Depending on the problem, this can make the explanations more powerful. However, interpreting the explanations can become increasingly challenging.

4.6. Extended learning curves

Two types of learning curves appears in literature. The first type visualizes the performance of an iterative machine learning algorithm as a function of its training time or number of iterations. The second type, which we concentrate on, is used to extrapolate performance from smaller to larger datasets (Domhan et al., 2015). Usually, the number of samples are shown on the horizontal axis, and the vertical axis shows a metric for the predictive power, for example mean squared error. Patterns which depend on the size of the training dataset are sometimes evident across different datasets, and such patterns can be discovered through learning curve analysis (Perlich et al., 2003; Kolachina et al., 2012).

When learning curves are drawn, the underlying training data is often grown only once. However, growing the dataset in a different way, will sometimes significantly change the shape of the learning curve. This information is typically not conveyed by traditional learning curves. When we calculate our Shapley values, the model is retrained M times, using different training datasets of different size. We can plot this information in a scatter plot, similar to a traditional learning curve, with size of training data on the horizontal axis, and the performance metric on the vertical axis. By doing this, more information about the data and the algorithm's learning process can be disclosed

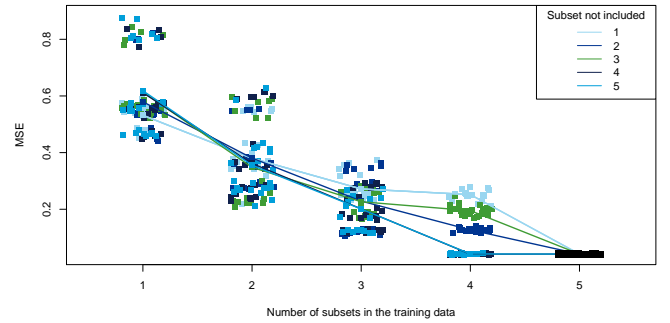


Figure 16: Extended learning curve for the time series example presented in Section 3.1.

to the user, which can enable more informed and possibly more accurate decisions.

Figure 16 shows an extended learning curve for the time series example presented in Section 3.1. When the five Shapley values for training data subset importance for squared error are approximated, for each iteration in the approximation procedure, new models are retrained on training data of different sizes. We calculate and store the mean squared error for the full test dataset on each iteration. These values are plotted in Figure 16, where the horizontal axis is the number of training data subsets used to train the model. In this example, all subsets are equal in size. For ease of visualization, we add some noise in the horizontal values. We show results from 100 iterations ($M = 100$). The training datasets comprise one or more subsets. The colors indicate which of the subsets of the training data are not included in the training dataset. For example, the results marked in light blue, are produced using datasets which comprise different coalitions of the subsets of the training data except subset 1. At five in the horizontal direction, the full training dataset (the coalition which comprises all subsets) is used for training. To ease readability, the results can be summarized in different ways. Here, we calculate the mean of the results at each point on the horizontal axis, and draw a line through these.

The extended learning curves proposed here can be used to visualize the learning process, by studying how including a subset in the training data affects the MSE. Careful analysis of the learning curves can contribute to increased understanding of the algorithm's inner workings, and be useful when assessing the robustness of the model. In the example presented in Figure 16, we can for example observe that including more data generally decrease the mean squared error. We can also, for example, observe that including all subsets except subset 4, gives approximately the same MSE as we obtain if subset 4 is included in the training data (see the black cluster at (4, 0.05)). This is not surprising since we know that subset 4 and 5 are identical. Including subset 1 (in addition to the four other subsets) does however lead to significant reduction of MSE (see the light blue cluster at (4, 0.2)). We can also

observe that a model based on training data consisting of one subset only gets a MSE between 0.4 and 0.6, except when subset 1 is included. We see this, since the cluster at (1, 0.8) does not include any light blue markers,

5. Conclusion

In this paper, we have proposed a novel model-agnostic methodology to explain individual predictions from black-box machine learning models. The proposed methodology quantifies how different subsets in the training data affect individual predictions. Two variants are presented: The first explains how subsets of the training data contribute to decrease or increase a prediction, and the second focus on the squared error.

The explanations give valuable insight into how the predictions are made and affected by the training data. This is insight which would not be available without the proposed methodology, and should complement the existing explanations offered by measures of feature importance.

We have devoted some attention to describing the importance of interpretation and explanations, and we argue that understanding the algorithms reasoning can provide trust. In some safety critical applications, interpretations and explanations can be seen as a prerequisite. This is also the case in many applications involving personal data, both due to regulations and public opinion.

To demonstrate the usefulness of the proposed methodology, we have carefully selected multiple illustrating examples, and used these to demonstrate and explain how the Shapley values for training data subset importance can be used. We have demonstrated that predictions of data with a known signal generating function are accurately explained. We have presented examples with simple and transparent models which we intuitively understand, and shown that the explanations provided by the Shapley values for subset importance correspond to intuitive explanations. We have also shown examples of how the Shapley values can be used to reveal biased behaviour and erroneous training data. Furthermore, we have suggested an improved data acquisition technique where more data is selected from the subset associated with high Shapley values. With the proposed approach, we were able to significantly reduce prediction error. This indicates that the explanations provided by the Shapley value for subset importance are in accordance with the intuitive expectation; that the most important subsets, the subsets with high Shapley values, contribute the most to reduce prediction error.

The novel approach proposed in this paper allows us to explore and investigate how the training data affects the predictions made by any black-box model. New aspects of the reasoning and inner workings of a prediction model and learning method can be conveyed.

Acknowledgements

The authors greatly appreciate the suggestions and criticisms by Odin Gramstad (DNV GL), Martin Jullum (Norwegian Computing Center), Arnoldo Frigessi (University of Oslo), Mette Langaas (Norwegian University of Science and Technology), Knut Erik Knutsen (DNV GL) and Erik Vanem (DNV GL/University of Oslo).

The work is carried out in collaboration with the Big Insight project, and is partly funded by the Research Council of Norway, project number 237718 and 251396.

References

Aas, K., Jullum, M., and Løland, A. (2019). Explaining individual predictions when features are dependent: More accurate approximations to shapley values. *arXiv preprint arXiv:1903.10464*.

Angwin, J., Larson, J., Mattu, S., and Kirchner, L. (2016). Machine bias. *ProPublica, May*, 23:2016.

Breiman, L. (2001). Random forests. *Machine learning*, 45(1):5–32.

Buolamwini, J. and Gebru, T. (2018). Gender shades: Intersectional accuracy disparities in commercial gender classification. In Friedler, S. A. and Wilson, C., editors, *Proceedings of the 1st Conference on Fairness, Accountability and Transparency*, volume 81 of *Proceedings of Machine Learning Research*, pages 77–91, New York, NY, USA. PMLR.

Caruana, R., Kangarloo, H., Dionisio, J., Sinha, U., and Johnson, D. (1999). Case-based explanation of non-case-based learning methods. In *Proceedings of the AMIA Symposium*, page 212. American Medical Informatics Association.

Castro, J., Gómez, D., and Tejada, J. (2009). Polynomial calculation of the shapley value based on sampling. *Computers & Operations Research*, 36(5):1726 – 1730. Selected papers presented at the Tenth International Symposium on Locational Decisions (ISOLDE X).

Çetiner, D. (2013). *Selected Topics in Cooperative Game Theory*, pages 43–72. Springer Berlin Heidelberg, Berlin, Heidelberg.

Cook, R. D. (1977). Detection of influential observation in linear regression. *Technometrics*, 19(1):15–18.

Cook, R. D. (1979). Influential observations in linear regression. *Journal of the American Statistical Association*, 74(365):169–174.

Dehez, P. (2015). On harsanyi dividends and asymmetrid values.

DNV GL (2017). Environmental conditions and environmental loads. *Recommended Practice DNVGL-RP-C205*.

Domhan, T., Springenberg, J. T., and Hutter, F. (2015). Speeding up automatic hyperparameter optimization of deep neural networks by extrapolation of learning curves. In *Twenty-Fourth International Joint Conference on Artificial Intelligence*.

Doshi-Velez, F. and Kim, B. (2017). Towards a rigorous science of interpretable machine learning. *arXiv preprint arXiv:1702.08608*.

Fanaee-T, H. and Gama, J. (2013). Event labeling combining ensemble detectors and background knowledge. *Progress in Artificial Intelligence*, pages 1–15.

Fisher, A., Rudin, C., and Dominici, F. (2018). All models are wrong but many are useful: Variable importance for black-box, proprietary, or misspecified prediction models, using model class reliance. *arXiv preprint arXiv:1801.01489*.

Goodman, B. and Flaxman, S. (2017). European union regulations on algorithmic decision-making and a “right to explanation”. *AI Magazine*, 38(3):50–57.

Hall, P. and Gill, N. (2018). *Introduction to Machine Learning Interpretability*. O'Reilly Media, Incorporated.

Harsanyi, J. C. (1963). A simplified bargaining model for the n-person cooperative game. *International Economic Review*, 4(2):194–220.

Kim, B., Khanna, R., and Koyejo, O. O. (2016). Examples are not enough, learn to criticize! criticism for interpretability. In *Advances in Neural Information Processing Systems*, pages 2280–2288.

Koh, P. W. and Liang, P. (2017). Understanding black-box predictions via influence functions. In *Proceedings of the 34th International Conference on Machine Learning-Volume 70*, pages 1885–1894. JMLR.org.

Kolachina, P., Cancedda, N., Dymetman, M., and Venkatapathy, S. (2012). Prediction of learning curves in machine translation. In *Proceedings of the 50th Annual Meeting of the Association for Computational Linguistics: Long Papers-Volume 1*, pages 22–30. Association for Computational Linguistics.

Liaw, A. and Wiener, M. (2002). Classification and regression by randomforest. *R News*, 2(3):18–22.

Lipovetsky, S. and Conklin, M. (2001). Analysis of regression in game theory approach. *Applied Stochastic Models in Business and Industry*, 17(4):319–330.

Lum, K. and Isaac, W. (2016). To predict and serve? *Significance*, 13(5):14–19.

Lundberg, S. M. and Lee, S.-I. (2017). A unified approach to interpreting model predictions. In *Advances in Neural Information Processing Systems*, pages 4765–4774.

Molnar, C. (2019). *Interpretable Machine Learning*. <https://christophm.github.io/interpretable-ml-book/>.

Molnar, C., Bischl, B., and Casalicchio, G. (2018). iml: An r package for interpretable machine learning. *JOSS*, 3(26):786.

Oberhagemann, J., Ervik, A. K., Gramstad, O., Helmers, J. B., Kaufmann, J., and Sireta, F.-X. (2019). Wave load and response predictions combining HOSM, CFD, and machine learning. In *ASME 2019 38th International Conference on Ocean, Offshore and Arctic Engineering*. American Society of Mechanical Engineers.

Perlich, C., Provost, F., and Simonoff, J. S. (2003). Tree induction vs. logistic regression: A learning-curve analysis. *Journal of Machine Learning Research*, 4(Jun):211–255.

R Core Team (2019). *R: A Language and Environment for Statistical Computing*. R Foundation for Statistical Computing, Vienna, Austria.

Ribeiro, M. T., Singh, S., and Guestrin, C. (2016). Why should I trust you?: Explaining the predictions of any classifier. In *Proceedings of the 22nd ACM SIGKDD international conference on knowledge discovery and data mining*, pages 1135–1144. ACM.

Shapley, L. S. (1953). A value for n-person games. *Contributions to the Theory of Games*, 2(28):307–317.

Shrikumar, A., Greenside, P., Shcherbina, A., and Kundaje, A. (2016). Not just a black box: Learning important features through propagating activation differences. *arXiv preprint:1605.01713*.

Strumbelj, E. and Kononenko, I. (2010). An efficient explanation of individual classifications using game theory. *Journal of Machine Learning Research*, 11(1).

Strumbelj, E. and Kononenko, I. (2011). A general method for visualizing and explaining black-box regression models. In *International Conference on Adaptive and Natural Computing Algorithms*, pages 21–30. Springer.

Strumbelj, E. and Kononenko, I. (2014). Explaining prediction models and individual predictions with feature contributions. *Knowledge and Information Systems*, 41(3):647–665.

Appendix A. Exact Shapley values

We recommend the following example to readers who aim to implement the proposed methodology and pursue a comprehensive overview of the technicalities. We consider a trivial toy-example where we derive the exact Shapley values for training data importance and explain the calculations step by step. The Shapley values are calculated for two simple regression models, and the exact and the approximated values are compared.

We divide the training dataset into three subsets, Q_1 , Q_2 and Q_3 . In order to derive and explain the exact calculations, we choose to use a trivial example and only con-

sider one explanatory variable x , and let the response y be equal to the explanatory variable x . Furthermore, we let the explanatory variables be

$$x_i \sim \begin{cases} 1/8 & \text{for } i \in Q_1 \\ 6/8 & \text{for } i \in Q_2 \\ 7/8 & \text{for } i \in Q_3 \end{cases} \quad (\text{A.1})$$

We evaluate two different nearest neighbour regression models, and calculate the associated Shapley values for both models. We denote the first model 1NN, which is a nearest neighbour model where we only consider the one nearest neighbour. The second model is denoted allNN, which is a model which outputs the mean of all neighbours. It is of course not common to include all neighbours, but this model serves the purpose well here, because it is simple to calculate and it illustrates the concept well. Furthermore, we let $f_\emptyset = 0$ in both cases, and evaluate one new data point $x^{new} = 2/8$, and calculate the Shapley values for the prediction of this data point only.

Appendix A.1. Shapley values expressed with Harsanyi dividends

In addition to the formulations (1) and (2), the Shapley values can be expressed using *Harsanyi dividends*. A Harsanyi dividend identifies the surplus that is created by a coalition of players in a coalitional game, corrected by the surplus that is already created by subcoalitions (Harsanyi, 1963; Dehez, 2015). A dividend may also be negative, that is it reduce the payouts of its members. The dividends are defined recursively as

$$\begin{aligned} d_v(\emptyset) &= 0 \\ d_v(\{i\}) &= v(\{i\}) \\ d_v(\{i, j\}) &= v(\{i, j\}) - d_v(\{i\}) - d_v(\{j\}) \\ d_v(\{i, j, k\}) &= v(\{i, j, k\}) - d_v(\{i, j\}) - d_v(\{i, k\}) - d_v(\{j, k\}) \\ &\quad - d_v(\{i\}) - d_v(\{j\}) - d_v(\{k\}) \\ &\vdots \\ d_v(S) &= v(S) - \sum_{T \subsetneq S} d_v(T). \end{aligned} \quad (\text{A.2})$$

The Harsanyi dividends are useful when analysing both games and solution concepts, and the division of payout that results from the equal division of dividends within each coalition coincides with the Shapley values (Dehez, 2015). That is, the Shapley value φ of a player i in game $\langle N, v \rangle$ can be expressed as

$$\varphi_i = \sum_{S \subset N: i \in S} \frac{d_v(S)}{|S|}. \quad (\text{A.3})$$

In the following, we calculate the Shapley values for the example presented above, using Harsanyi dividends.

The Harsanyi dividends are displayed in Table A.1. Note that when we calculate $d_v(1, 2)$ in table A.1, for the 1NN model, we use that

$$\begin{aligned} d_v(1, 2) &= v(1, 2) - d_v(1) - d_v(2) \\ &= d_v(1) - d_v(1) - d_v(2) \\ &= -d_v(2). \end{aligned} \quad (\text{A.4})$$

We know that $v(1, 2) = v(1)$ since the predictions will not change by adding data from subset 2. Whenever data from subset 1 is included in the training dataset, the prediction will always be equal to the data in subset 1, which is $1/8$. Similarly, we use that $v(1, 3) = d_v(1)$ to calculate $d_v(1, 3)$, and we use that $v(2, 3) = d_v(2)$ to calculate $d_v(2, 3)$.

When we use the *allNN* model, this is not the case, because now all points in the training data are equally important, and hence

$$\begin{aligned} d_v(1, 2) &= v(1, 2) - d_v(1) - d_v(2) \\ &= (v(1) + v(2))/2 - v(1) - v(2) \\ &= (1/8 + 6/8)/2 - 1/8 - 6/8 \\ &= -8/16. \end{aligned} \quad (\text{A.5})$$

The Shapley values are calculated in Table A.2.

Appendix A.2. Shapley values based on average marginal contributions

Here, we calculate the Shapley values by averaging over the marginal distributions with respect to all the permutations. We have $K = 3$ subsets, which gives $3! = 6$ possible permutations. These are listed in the first column of Table A.3-A.8. Values related to the 1NN method are provided in Table A.3 - A.5. The values related to the *allNN* method are provided in Table A.6 - A.8. In the second and third column of the tables, the accompanying subsets $S \cup \{k\}$ and S are listed. In column four and five, the exact predictions are written, and difference between them are expressed in the sixth column.

Following (1), we sum the differences, and divide by $K!$. This gives the exact Shapley values as presented in Table A.9.

Appendix A.3. Efficiency of the Shapley values

Now we demonstrate that the exact solution provided above satisfies the efficiency property. The other properties are of course also satisfied, but for space limitations, we do not show this for this example. We remember that according to the efficiency property, the total gain is distributed. That is, the sum of the Shapley values is equal to the worth of the grand coalition.

For the 1NN model we have that

$$v(N)(x) = E[f_N(x)] = \frac{1}{8} \quad (\text{A.6})$$

and

$$\sum_{k \in N} \varphi_k = \frac{-19}{48} + \frac{11}{48} + \frac{14}{48} = \frac{1}{8}, \quad (\text{A.7})$$

Similarly, for the *allNN* model, we have that

$$v(N)(x) = E[f_N(x)] = \frac{7}{12} \quad (\text{A.8})$$

and

$$\sum_{k \in N} \varphi_k = \frac{-43}{288} + \frac{92}{288} + \frac{119}{288} = \frac{7}{12}. \quad (\text{A.9})$$

In both cases we see that

$$\sum_{k \in N} \varphi_k(v) = v(N). \quad (\text{A.10})$$

Appendix A.4. Approximated Shapley values

We also approximate the Shapley values using the methodology presented in 2.3, with $M = 250$ Monte Carlo iterations. The approximated Shapley values of $x^{new} = 2/8$ are presented in Table A.10.

We observe that this corresponds well with the exact values presented in Table A.2.

Appendix A.4.1. Example

As an example, we calculate the approximated Shapley values for a grid of values for $x^{new} \in (0, 1)$. In Figure A.17a and A.17b we have used the 1NN and the *allNN* models as described above. Figure A.17c and A.17d show the approximated Shapley values for predictions made with linear regression and a random forest model with 10 trees. The values x^{new} are shown in black, and associated predictions are shown in red, with true values along the horizontal axis, and predicted values along the vertical axis. The Shapley values of subset 1, 2 and 3 are shown in light blue, blue and green, for observations along the horizontal axis.

Harsanyi	Calculations	1NN	<i>all</i> NN
$d_v(1)$	$v(1)$	1/8	1/8
$d_v(2)$	$v(2)$	6/8	6/8
$d_v(3)$	$v(3)$	7/8	7/8
$d_v(1, 2)$	$v(1, 2) - d_v(1) - d_v(2)$	-6/8	-7/16
$d_v(1, 3)$	$v(1, 3) - d_v(1) - d_v(3)$	-7/8	-8/16
$d_v(2, 3)$	$v(2, 3) - d_v(2) - d_v(3)$	-7/8	-13/16
$d_v(1, 2, 3)$	$v(1, 2, 3) - d_v(1, 2) - d_v(1, 3) - d_v(2, 3) - d_v(1) - d_v(2) - d_v(3)$	7/8	7/12

Table A.1: Harsanyi dividends for the trivial example presented in Appendix A.

Shapley value	Calculations	1NN	<i>all</i> NN
φ_1	$d_v(1) + \frac{1}{2} \cdot d_v(1, 2) + \frac{1}{2} \cdot d_v(1, 3) + \frac{1}{3} \cdot d_v(1, 2, 3)$	$\frac{-19}{48} \approx -0.396$	$\frac{-43}{288} \approx -0.149$
φ_2	$d_v(2) + \frac{1}{2} \cdot d_v(1, 2) + \frac{1}{2} \cdot d_v(2, 3) + \frac{1}{3} \cdot d_v(1, 2, 3)$	$\frac{11}{48} \approx 0.229$	$\frac{92}{288} \approx 0.319$
φ_3	$d_v(3) + \frac{1}{2} \cdot d_v(1, 3) + \frac{1}{2} \cdot d_v(2, 3) + \frac{1}{3} \cdot d_v(1, 2, 3)$	$\frac{14}{48} \approx 0.292$	$\frac{119}{288} \approx 0.413$

Table A.2: Shapley values for the trivial example presented in Appendix A.

\mathcal{O}	$S \cup \{k\}$	S	$f_{\mathcal{O} \cup \{i\}}$	$f_{\mathcal{O}}$	$f_{\mathcal{O} \cup \{k\}} - f_{\mathcal{O}}$
{1 2 3}	{1}	\emptyset	1/8	0	1/8
{1 3 2}	{1}	\emptyset	1/8	0	1/8
{2 1 3}	{1, 2}	{2}	1/8	6/8	-5/8
{2 3 1}	{1, 2, 3}	{2, 3}	1/8	6/8	-5/8
{3 1 2}	{1, 3}	{3}	1/8	7/8	-3/4
{3 2 1}	{1, 2, 3}	{2, 3}	1/8	6/8	-5/8

Table A.3: **1NN - subset 1:** Calculation of the exact Shapley Value for Subset Importance of subset 1, using model 1NN, for the problem presented in Appendix A.

\mathcal{O}	$S \cup \{k\}$	S	$f_{\mathcal{O} \cup \{i\}}$	$f_{\mathcal{O}}$	$f_{\mathcal{O} \cup \{i\}} - f_{\mathcal{O}}$
{1 2 3}	{1, 2}	{1}	1/8	1/8	0
{1 3 2}	{1, 2, 3}	{1, 3}	1/8	1/8	0
{2 1 3}	{2}	\emptyset	6/8	0	6/8
{2 3 1}	{2}	\emptyset	6/8	0	6/8
{3 1 2}	{1, 2, 3}	{1, 3}	1/8	1/8	0
{3 2 1}	{2, 3}	{3}	6/8	7/8	-1/8

Table A.4: **1NN - subset 2:** Calculation of the exact Shapley Value for Subset Importance of subset 2, using model 1NN, for the problem presented in Appendix A.

\mathcal{O}	$S \cup \{k\}$	S	$f_{\mathcal{O} \cup \{i\}}$	$f_{\mathcal{O}}$	$f_{\mathcal{O} \cup \{i\}} - f_{\mathcal{O}}$
{1 2 3}	{1, 2, 3}	{1, 2}	1/8	1/8	0
{1 3 2}	{1, 3}	{1}	1/8	1/8	0
{2 1 3}	{1, 2, 3}	{1, 2}	1/8	1/8	0
{2 3 1}	{2, 3}	{2}	6/8	6/8	0
{3 1 2}	{3}	\emptyset	7/8	0	7/8
{3 2 1}	{3}	\emptyset	7/8	0	7/8

Table A.5: **1NN - subset 3:** Calculation of the exact Shapley Value for Subset Importance of subset 3, using model 1NN, for the problem presented in Appendix A.

\mathcal{O}	$S \cup \{k\}$	S	$f_{\mathcal{O} \cup \{i\}}$	$f_{\mathcal{O}}$	$f_{\mathcal{O} \cup \{k\}} - f_{\mathcal{O}}$
$\{1 2 3\}$	$\{1\}$	\emptyset	$(1/8 + 0 + 0)/1$	$(0 + 0 + 0)/3$	$1/8$
$\{1 3 2\}$	$\{1\}$	\emptyset	$(1/8 + 0 + 0)/1$	$(0 + 0 + 0)/3$	$1/8$
$\{2 1 3\}$	$\{1, 2\}$	$\{2\}$	$(1/8 + 6/8 + 0)/2$	$(0 + 6/8 + 0)/1$	$-5/16$
$\{2 3 1\}$	$\{1, 2, 3\}$	$\{2, 3\}$	$(1/8 + 6/8 + 7/8)/3$	$(0 + 6/8 + 7/8)/2$	$-11/48$
$\{3 1 2\}$	$\{1, 3\}$	$\{3\}$	$(1/8 + 0 + 7/8)/2$	$(0 + 0 + 7/8)/1$	$-3/8$
$\{3 2 1\}$	$\{1, 2, 3\}$	$\{2, 3\}$	$(1/8 + 6/8 + 7/8)/3$	$(0 + 6/8 + 7/8)/2$	$-11/48$

Table A.6: **allNN - subset 1:** Calculation of the exact Shapley Value for Subset Importance of subset 1, using model *allNN*, for the problem presented in Appendix A.

\mathcal{O}	$S \cup \{k\}$	S	$f_{\mathcal{O} \cup \{i\}}$	$f_{\mathcal{O}}$	$f_{\mathcal{O} \cup \{i\}} - f_{\mathcal{O}}$
$\{1 2 3\}$	$\{1, 2\}$	$\{1\}$	$(1/8 + 6/8 + 0)/2$	$(1/8 + 0 + 0)/1$	$5/16$
$\{1 3 2\}$	$\{1, 2, 3\}$	$\{1, 3\}$	$(1/8 + 6/8 + 7/8)/3$	$(1/8 + 0 + 7/8)/2$	$1/12$
$\{2 1 3\}$	$\{2\}$	\emptyset	$(0 + 6/8 + 0)/1$	$(0 + 0 + 0)/0$	$6/8$
$\{2 3 1\}$	$\{2\}$	\emptyset	$(0 + 6/8 + 0)/1$	$(0 + 0 + 0)/0$	$6/8$
$\{3 1 2\}$	$\{1, 2, 3\}$	$\{1, 3\}$	$(1/8 + 6/8 + 7/8)/3$	$(1/8 + 0 + 7/8)/2$	$1/12$
$\{3 2 1\}$	$\{2, 3\}$	$\{3\}$	$(0 + 6/8 + 7/8)/2$	$(0 + 0 + 7/8)/1$	$-1/16$

Table A.7: **allNN - subset 2:** Calculation of the exact Shapley Value for Subset Importance of subset 2, using model *allNN*, for the problem presented in Appendix A.

\mathcal{O}	$S \cup \{k\}$	S	$f_{\mathcal{O} \cup \{i\}}$	$f_{\mathcal{O}}$	$f_{\mathcal{O} \cup \{i\}} - f_{\mathcal{O}}$
$\{1 2 3\}$	$\{1, 2, 3\}$	$\{1, 2\}$	$(1/8 + 6/8 + 7/8)/2$	$(1/8 + 6/8 + 0)/2$	$7/48$
$\{1 3 2\}$	$\{1, 3\}$	$\{1\}$	$(1/8 + 7/8)/2$	$1/8$	$3/8$
$\{2 1 3\}$	$\{1, 2, 3\}$	$\{1, 2\}$	$(1/8 + 6/8 + 7/8)/3$	$(1/8 + 6/8)/2$	$7/48$
$\{2 3 1\}$	$\{2, 3\}$	$\{2\}$	$(0 + 6/8 + 7/8)/2$	$6/8$	$1/16$
$\{3 1 2\}$	$\{3\}$	\emptyset	$7/8$	0	$7/8$
$\{3 2 1\}$	$\{3\}$	\emptyset	$7/8$	0	$7/8$

Table A.8: **allNN - subset 3:** Calculation of the exact Shapley Value for Subset Importance of subset 3, using model *allNN*, for the problem presented in Appendix A.

Shapley values	1NN	<i>allNN</i>
φ_1	$\frac{-19/8}{3!} \approx -0.396$	$\frac{-43/48}{3!} \approx -0.149$
φ_2	$\frac{11/8}{3!} \approx 0.229$	$\frac{23/12}{3!} \approx 0.319$
φ_3	$\frac{14/8}{3!} \approx 0.292$	$\frac{119/48}{3!} \approx 0.413$

Table A.9: Shapley values calculated by averaging over the marginal distributions with respect to all the permutations, for the trivial example presented in Appendix A.

Approximate Shapley value	1NN	<i>allNN</i>
$\hat{\varphi}_1$	-0.432	-0.170
$\hat{\varphi}_2$	0.229	0.324
$\hat{\varphi}_3$	0.308	0.431

Table A.10: Approximated Shapley values for the trivial example presented in Appendix A.

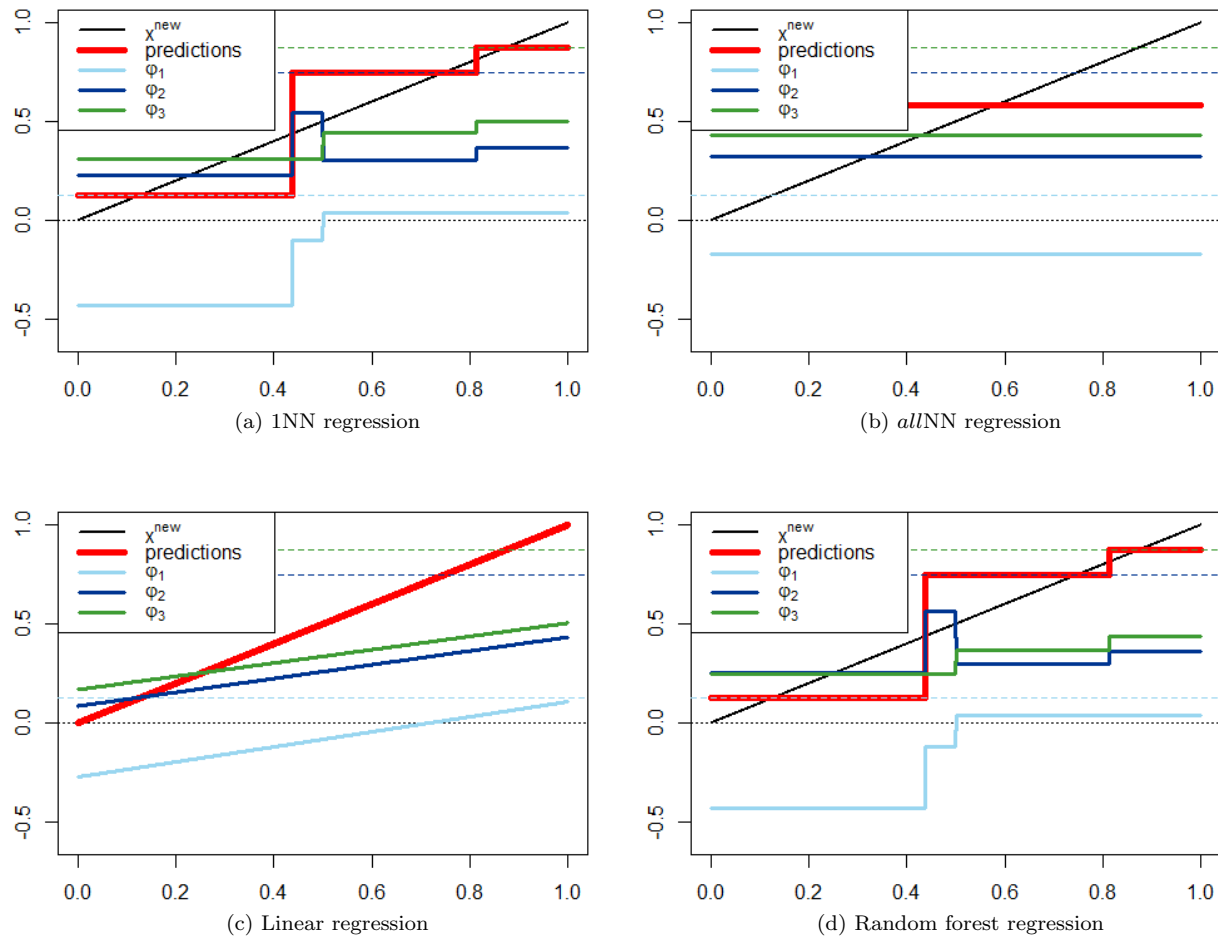


Figure A.17: Approximated Shapley values